Simulation of point vortex system and Onsager's "negative temperature" theory of 2D turbulence

A THESIS
SUBMITTED TO THE FACULTY OF THE GRADUATE SCHOOL
OF THE UNIVERSITY OF MINNESOTA
BY

Su Liang

IN PARTIAL FULFILLMENT OF THE REQUIREMENTS
FOR THE DEGREE OF
MASTER OF SCIENCE

Advisor: Hao Jia

December, 2020

Acknowledgements

There are many people that have earned my gratitude for their contribution to my time in graduate school. First, I'm extremely grateful to my advisor, Prof. Hao Jia, for his guidance and support. It was a happy and pressureless time to research with him, and I learned a lot from his mathematical intuition and rigorous research style. Without his help, I might not have the chance to step into the academic world of Mathematics.

I am grateful to Prof. Vladimir Sverak and Prof. Joseph Nichols, for serving as my committee members. I am also grateful to Prof. Max Engelstein, for helping me with the application. Their lectures are also very good, and I learned a lot from their academic style.

I would like to thank Prof. Chris Hogan, Prof. Ru-Yu Lai, Prof. Matt Anderson, Ms. Bonny Fleming and Prof. Richard McGehee, for their kind help when I was trying to change my program of study. That period of time was tough for me, and they let me realize there are so many kind people around me.

Special thanks to Dingbin Huang, Jinwei Yang, Mingxiang Zhao, Hongyuan Zhang, for their support and encouragement. The time with them is pleasant and I value our friendship.

Abstract

For 2D turbulence, a commonly-observed phenomenon is the formation of large structure vortices, such as the Great Red Spot in the upper atmosphere of Jupiter, where the flow is approximately two dimensional. Lars Onsager proposed such phenomenon "suggests an explanation on statistical grounds" (1949). He tried to use statistical mechanics to analyze 2D point vortices system, and came up with the idea of "negative temperature" to describe the clustering of vortices. This thesis focuses on this novel "negative temperature" concept, and uses both numerical simulation and theoretical analysis to explain it. Here, we develop a numerical method to simulate the evolution of point vortices in a periodic square. Our simulation shows that point vortices system could capture the phenomenon of the coalescence of same sign vortices. However, it requires specific set-up of the distribution of initial vortices. We observe that such distribution has high energy in the Hamiltonian sense, and usually already has some small structures of clustering of vortices. By analyzing its phase space, we find that the entropy of such distribution will decrease as energy grows, which is consistent with the concept of "negative temperature". We also discover other distributions of point vortices that have different properties from the "negative temperature" case, which we call "infinity temperature" and "positive temperature". Our simulation shows this "positive temperature" and "negative temperature" can neutralize each other. By following the "temperature" idea, we can regard the coalescence of same sign vortices as the balancing of temperature. In the last chapter, we analyze the structure of the phase space of the point vortices system, and proposed a new idea of "energy shell thickness" to explain the coalescence of same sign vortices.

Contents

Acknowledgements **i**

Abstract **ii**

List of Tables **v**

List of Figures **vi**

1 Introduction **1**

2 Statistical mechanics on point vortex system **5**

2.1 2D Euler and point vortex system 5

2.2 Point vortex system on the periodic square (torus) 8

2.3 Microcanonical ensemble of point vortices system 11

2.3.1 Microcanonical ensemble 11

2.3.2 Negative temperature for point vortices system 13

2.4 The interpretation of negative temperature 14

3 Numerical method **18**

3.1 Algorithm of the velocity of point vortex in periodic square 18

3.1.1 The velocity generated by one cell 19

3.1.2 Summation of the velocity generated by cells 23

3.2 Time advancement 25

4 Simulation results **28**

4.1 Infinity temperature 28

4.1.1 Case 1: randomly distributed point vortices in a torus 28
4.1.2 Phase space analysis 28
4.2 Negative temperature 30
4.2.1 Case 2: two opposite sign vortex patches will never merge 31
4.2.2 The energy difference between case 1 and case 2 31
4.2.3 Case 3: 2D turbulence 33
4.2.4 Coexistence of negative and infinity temperature 34
4.3 Negative temperature in $\mathbb{R}^2$ 38
4.3.1 Case 4: merging of two co-rotating vortex patches 38
4.3.2 The irreversibility of merging 40
4.3.3 Case 5: merging of many vortex patches 41
4.4 Positive temperature 43
4.4.1 Case 6: many dipoles 43
4.4.2 Case 7: free expansion 45
4.4.3 Case 8: neutralization of positive temperature and negative temperature 47

5 A new point of view: energy shell thickness **50**
5.1 The simplest example 51
5.2 Energy shell thickness 54
5.3 Three vortices in 1D 55
5.4 Four vortices in 1D 58
5.5 Many vortices in 2D 58

6 Conclusion **61**

References **63**

Appendix A. The Taylor expansions of terms in equation (3.9) (3.10) **65**

Appendix B. Figures of evolution of 2D turbulence **79**

List of Tables

3.1 Taylor expansion of the integrand function of velocity. 19
3.2 Velocity on point (x, y) generated by the (i, j)th cell 21
3.3 Change of distance between two equal vortices rotate in a circle 26
4.1 The number of dipoles in which the distance of vortex pair is small (time 100 in case 6 v.s. time 100 in case 1) 45
4.2 The number of dipoles in which the distance of vortex pair is small, at time 100 in case 6, case 1, case 8 47
A.1 Expansion of u^x_{out} and u^y_{out} with coefficient M_x 65
A.2 Expansion of u^x_{out} and u^y_{out} with coefficient M_y 67
A.3 Expansion of u^x_{out} and u^y_{out} with coefficient M_{x^2} 69
A.4 Expansion of u^x_{out} and u^y_{out} with coefficient M_{xy} 70
A.5 Expansion of u^x_{out} and u^y_{out} with coefficient M_{y^2} 71
A.6 Expansion of u^x_{out} and u^y_{out} with coefficient M_{x^3} 72
A.7 Expansion of u^x_{out} and u^y_{out} with coefficient M_{x^2y} 73
A.8 Expansion of u^x_{out} and u^y_{out} with coefficient M_{xy^2} 74
A.9 Expansion of u^x_{out} and u^y_{out} with coefficient M_{y^3} 75
A.10 Expansion of u^x_{out} and u^y_{out} with coefficient M_{x^4} 76
A.11 Expansion of u^x_{out} and u^y_{out} with coefficient M_{x^3y} 76
A.12 Expansion of u^x_{out} and u^y_{out} with coefficient $M_{x^2y^2}$ 77
A.13 Expansion of u^x_{out} and u^y_{out} with coefficient M_{xy^3} 77
A.14 Expansion of u^x_{out} and u^y_{out} with coefficient M_{y^4} 78

List of Figures

2.1 Enegy shell 12
2.2 Schematic diagram of the phase space volume $\Omega(E)$ of point vortices system in a torus 14
2.3 Schematic diagram of the derivative of phase space volume $\Omega'(E)$ of point vortices system in a torus 15
2.4 Schematic diagram of the inverse temperature $\beta = \Omega'(E)/\Omega(E)$ of point vortices system in a torus 15
2.5 Schematic diagram of the temperature $T = 1/\beta = \Omega(E)/\Omega'(E)$ of point vortices system in a torus 16
4.1 Randomly distributed 2000 vortices in a torus; after developing for 100 dimensionless time 29
4.2 2000 vortices, with same sign vortices clustered in a circle; after developing for 100 dimensionless time 32
4.3 100 small vortex patches (50 positive and 50 negative), with each patch contains 20 point vortices; after developing for 200 dimensionless time . 35
4.4 The final distribution of 2D turbulence case 37
4.5 2 big vortex patch circles, each with 1000 point vortices inside, at time 0, 0.4, 0.6, 0.8, 1, 20 39
4.6 Schematic diagram of the 3 systems of two big vortex patches 40
4.7 1000 vortices, forming 50 small vortex patches; after developing for 100 dimensionless time 42
4.8 1000 vortex dipoles in torus; after developing for 100 dimensionless time 44
4.9 Free expansion of randomly distributed vortices in a small square, at time 0, 1, 5, 10, 50, 100 46

4.10 2000 vortices, with 1750 in the left domain forming dipole, and 250 in the right domain forming vortex patches; after developing for 100 dimensionless time 49
5.1 Energy shell. 50
5.2 Phase space of two vortices system in 1D; the blue line quantifies the thickness of energy shell. 52
5.3 Phase space volume $\Omega(E)$ of two vortices system in 1D 53
5.4 Schematic diagram of the method to quantify the thickness of energy shell 55
5.5 Function of $d_1(h_1)$ and $d_2(h_1)$ 57
5.6 The most probable state of three vortices in 1D 57
5.7 The most probable state of four vortices in 1D 58
5.8 Evolution to most probable state 59
5.9 Vortex patch in the shape of ring in $\mathbb{R}^2$, at time 0, 2, 5, 10, 20, 50 . . . 60
B.1 2D turbulence on torus, at time 0, 1, 2, 5, 10, 20 80
B.2 2D turbulence on torus, at time 30, 40, 50, 100, 150, 200 81

Chapter 1

Introduction

2D turbulence often concerns the long time behavior of the two dimensional fluid flows with no boundary condition, such as in $\mathbb{R}^2$ or in a periodic domain. A prominent feature of such flows is the formation of large scale vortices. There are many relevant phenomenon in our natural world of 2D turbulence, e.g., the formation of hurricane. Since our atmosphere has the thickness of a few tens of kilometers, while the lateral extent is tens of thousands of kilometers, in many cases we can use 2D fluid flow equations to analyze the formation and evolution of hurricane [1]. Another example is the long-lived Great Red Spot in the upper atmosphere of Jupiter [2], which is several times the size of the earth, and has lasted for at least 180 years. In this thesis, our main object is to study such formation of large structure vortices in 2D turbulence.

Though we use the term "turbulence" to name such 2D fluid flow, it has completely different properties from the 3D turbulence. For fully developed 3D turbulence, we have the widely accepted Kolmogorov's hypothesis, which states the small-scale turbulent motions are statistically isotropic. This isotropy can define a universal equilibrium range, which could also be splitted into inertial subrange and dissipation range. In the inertial subrange our energy spectrum should satisfy the "-5/3 law", and in the dissipation range our kinetic energy will be dissipated [3]. The above concepts depict the picture of "energy cascade", which states that the energy will flow from large scales to small scales, and finally dissipate in the smallest scales. In contrast, for 2D turbulence, there is no such isotropy (at least as observed in numerical simulation or experiment), thus no such universal equilibrium range. Also, in 2D there is no vortex stretching,

which may be a key mechanism to move energy from large scales to small scales in 3D, and consequently there is no direct energy cascade. Instead, 2D turbulence exhibits a so called "inverse energy cascade" [4], which states that the energy will flow from small scales to large scales.

To dig deeper into this "inverse energy cascade", we can look at the relationship between energy and enstrophy. For 2D periodic domain, any divergent term will disappear after integrating in the whole domain. Hence the 2D N-S equation may give us:

$$\frac{dE}{dt} = -2\nu\Omega \tag{1.1}$$

$$\frac{d\Omega}{dt} = -2\nu P \tag{1.2}$$

where $E = \langle \frac{1}{2}\boldsymbol{u}^2 \rangle$ is the kinetic energy, $\boldsymbol{u}$ is the velocity, $\Omega = \langle \frac{1}{2}\omega^2 \rangle$ is the enstrophy, ω is the vorticity, $P = \langle |\nabla\omega|^2 \rangle$ is named palinstrophy, and $\langle ... \rangle$ represents a spatial average. Since $P \geq 0$, from equation (1.2), we can see the enstrophy will only decrease with time, hence is bounded. Then from equation (1.1), we can see as viscosity $\nu \to 0$, the energy dissipation rate $\frac{dE}{dt} \to 0$. The boundedness of enstrophy is only featured in 2D flow, since in 3D the enstrophy could be amplified by vortex stretching, resulting in finite energy dissipation in the limit of vanishing viscosity [5]. Hence, for large Reynolds number flow in 2D, the energy cannot be dissipated quickly enough by viscosity, and it could be transfered to large scales by the inverse cascade. Phenomenally, we will see the formation of large scale vortices.

Besides the above rough analysis, Onsager has provided a different view to understand this inverse cascade in 2D turbulence. In his famous 1949 paper [6], Onsager wrote:
"The formation of large, isolated vortices is an extremely common, yet spectacular phenomenon in unsteady flow. Its ubiquity suggests an explanation on statistical grounds."

He used point vortex system to represent the actual continuous vorticity field. Then, he applied the statistical mechanics language (or tools) to analyze the system of point vortex, and found that in a confined domain, the phase space volume ($\Omega(E)$) of such system will decrease as energy grows, which means the entropy of such system will decrease as energy grows. Based on this observation, Onsager concludes that this system

has the "negative temperature" property. Meanwhile, he said this "negative temperature" could be used to explain the formation of large scale vortices:
"if $1/\Theta < 0$, then vortices of the same sign will tend to cluster, – preferably the strongest ones –, so as to use up excess energy at the least possible cost in terms of degrees of freedom. It stands to reason that the large compound vortices formed in this manner will remain as the only conspicuous features of the motion; because the weaker vortices, free to roam practically at random, will yield rather erratic and disorganised contributions to the flow."

The above explaination is highly concise. For many years after Onsager published his paper, there was no more explorations on this "negative temperature" idea [7]. In 1973, Joyce and Montgomery [8][9] derived a new meaningful and enlightening equation based on the idea of Onsager. They regard the vorticity as evenly distributed point vortices, and then use some combinatorial ideas to derive the expression of entropy of the system. By maximizing the entropy under the constraints of energy and total amount of vorticity, they get an equation for stream function:

$$-\Delta\psi = \exp\big(-\beta(\psi-\mu_+)\big) - \exp\big(\beta(\psi-\mu_-)\big) \tag{1.3}$$

where β, μ_+ and μ_- are the Lagrange multipliers of the energy, positive vorticity and negative vorticity constraint equations. This is very similar to Onsager's idea because they also use the point vortex system and the statistical mechanics point of view, and this coefficient β could be regarded as some kind of negative temperature.

If we believe the system will evolute in the direction of growing entropy which was derived by the combinatorics, we may get the final state of the evolution of point vortex system by solving equation (1.3). However, the correctness of Joyce and Montgomery' idea remains to be certified. In addition, it remains to be a problem if equation (1.3) can tell us any information of the evolution process rather than just the final state.

In this thesis, we carry out further study on the coalescence of same sign vortices in 2D turbulence based on Onsager's "negative temperature" idea. In chapter 2 we demonstrate the suitability of using point vortex system to represent the evolution of 2D Euler equation; we then analyze this system by using concepts in statistical mechanics.

In chapter 3 we describe our numerical method of solving point vortex system in a periodic domain. In chapter 4 we show the simulation results, and analyze the results. In chapter 5, we present a new idea based on "energy shell thickness" to understand the direction of evolution of point vortex system.

Chapter 2

Statistical mechanics on point vortex system

2.1 2D Euler and point vortex system

The 2D inviscid, incompressible fluid flow is governed by the 2D Euler's equation:

$$\frac{\partial \boldsymbol{u}}{\partial t} + \boldsymbol{u} \cdot \nabla \boldsymbol{u} + \frac{1}{\rho} \nabla p = 0 \tag{2.1}$$

$$\nabla \cdot \boldsymbol{u} = 0 \tag{2.2}$$

where $\boldsymbol{u}(\boldsymbol{x}, t)$ is the velocity field (here we assume $\boldsymbol{x} \in \mathbb{R}^2$), t is time, $p(\boldsymbol{x}, t)$ is the pressure, ρ is the density. Here we assume the density is a constant, which implies the incompressibility.

The vorticity is defined by:

$$\omega = -\nabla^{\perp} \cdot \boldsymbol{u} = -\frac{\partial u_1}{\partial x_2} + \frac{\partial u_2}{\partial x_1} \tag{2.3}$$

where $\nabla^{\perp} = (\frac{\partial}{\partial x_2}, -\frac{\partial}{\partial x_1})$. The vorticity ω satisfies the equation:

$$\frac{\partial \omega}{\partial t} + \boldsymbol{u} \cdot \nabla \omega = 0 \tag{2.4}$$

Since we have equation (2.2), we can define the stream function ψ of the velocity,

which satisfies:

$$\boldsymbol{u} = \nabla^{\perp}\psi = (\frac{\partial\psi}{\partial x_2}, -\frac{\partial\psi}{\partial x_1}) \tag{2.5}$$

and the vorticity is then given by:

$$\omega = -\Delta\psi \tag{2.6}$$

Hence, using the Green's function in $\mathbb{R}^2$, we can express ψ by:

$$\psi = \int_{\mathbb{R}^2} -\frac{1}{2\pi}\ln|\boldsymbol{x}-\boldsymbol{y}|\,\omega(\boldsymbol{y},t)\,d\boldsymbol{y} \tag{2.7}$$

And the velocity can also be expressed as:

$$\boldsymbol{u} = \nabla^{\perp}\psi = \int_{\mathbb{R}^2} -\frac{1}{2\pi}\frac{(\boldsymbol{x}-\boldsymbol{y})^{\perp}}{|\boldsymbol{x}-\boldsymbol{y}|^2}\,\omega(\boldsymbol{y},t)\,d\boldsymbol{y} \tag{2.8}$$

where $\boldsymbol{x}^{\perp} = (x_2, -x_1)$.

In 2D, it is well known that N-S equation approaches Euler equation as viscosity approaches zero in the absence of boundary. Therefore for many purposes, Euler equation is sufficient for us to capture the property of 2D turbulence. Also, it has been proved that for initial vorticity $\omega(\boldsymbol{x},0) \in L^1 \cap L^\infty$, there exists a unique solution $\omega(\boldsymbol{x},t) \in L^1 \cap L^\infty$, see e.g., [10].

In this thesis, we will not study the 2D Euler equation for general initial data. Instead, we will focus on point vortex system, whose evolution is very similar to Euler equation. In this system, we have N so-called point vortices in the position $\boldsymbol{x}_i(t) = (x_i(t), y_i(t)) \in \mathbb{R}^2$, with strength Γ_i, and their evolution satisfies:

$$\frac{d\boldsymbol{x}_i}{dt} = \sum_{\substack{j=1\\ j\neq i}}^{N} -\frac{1}{2\pi}\frac{(\boldsymbol{x}_i-\boldsymbol{x}_j)^{\perp}}{|\boldsymbol{x}_i-\boldsymbol{x}_j|^2}\Gamma_j \tag{2.9}$$

The system (2.9) is Hamiltonian with the Hamiltonian function given by:

$$\mathcal{H} = -\frac{1}{2\pi}\sum_{i<j}\Gamma_i\Gamma_j \ln|\boldsymbol{x}_i - \boldsymbol{x}_j| \tag{2.10}$$

then we have:

$$\Gamma_i \frac{dx_i}{dt} = \frac{\partial \mathcal{H}}{\partial y_i} \tag{2.11}$$

$$\Gamma_i \frac{dy_i}{dt} = -\frac{\partial \mathcal{H}}{\partial x_i} \tag{2.12}$$

One can easily check that the Hamiltonian is conserved during the evolution:

$$\begin{aligned}\frac{d\mathcal{H}}{dt} &= \sum_{i=1}^{N}\Big(\frac{\partial \mathcal{H}}{\partial x_i}\frac{dx_i}{dt} + \frac{\partial \mathcal{H}}{\partial y_i}\frac{dy_i}{dt}\Big) \\ &= \sum_{i=1}^{N}\frac{1}{\Gamma_i}\Big(\frac{\partial \mathcal{H}}{\partial x_i}\frac{\partial \mathcal{H}}{\partial y_i} - \frac{\partial \mathcal{H}}{\partial y_i}\frac{\partial \mathcal{H}}{\partial x_i}\Big) = 0\end{aligned} \tag{2.13}$$

There are cases in which singularities (two vortices collide with each other) happen, but it can be proved that the collapses are exceptional [11]. In most cases the Hamiltonian is well defined.

Marchioro and Pulvirenti [12] proved in 1993 that for vorticity blobs that are concentrated in many small areas, the evolution of these blobs according to 2D Euler equation is very close to the evolution of point vortex system. Specifically, if we have N vorticity blobs in $\mathbb{R}^2$ domain, with each of them contained in a small circle with radius ϵ, while the total vorticity of each blob is fixed (say Γ_i), and let this vorticity field evolve according to Euler equation, then for any given time $T > 0$ and length $d > 0$, there exists an $\epsilon > 0$ such that during the time in $[0, T]$, these blobs will still be contained in a small circle with radius d, and the centers of the circles are evolved according to the above point vortex system.

The above conclusion shows that point vortex system can approximate the evolution of concentrated vorticity blobs. As for continuous vorticity field, Marchioro and Pulvirenti [11] proved in Theorem 5.3.1 that any smooth solution $\omega(\boldsymbol{x}, t)$ of 2D Euler equation can be approximated by $\sum_{i=1}^{N} a_i\delta(\boldsymbol{x}_i(t))$ as $N \to \infty$, within the time $[0, T]$,

and these $\boldsymbol{x}_i(t)$ are evoluted according to point vortex system.

Hence, the point vortex system is a good approximation of 2D Euler equation, and it is reasonable to use it to study 2D turbulence. One concern is the above conclusions are all proved in $\mathbb{R}^2$, which assumes the vorticity decays in infinity, while our following studies are mostly in periodic square (torus). However, it is not difficult to see the analysis applies to our setting as well.

2.2 Point vortex system on the periodic square (torus)

Let our domain be a $[0,1)\times[0,1)$ square, and the velocity boundary condition is periodic in both x and y direction, that is:

$$\boldsymbol{u}(0,y) = \boldsymbol{u}(1,y) \tag{2.14}$$

$$\boldsymbol{u}(x,0) = \boldsymbol{u}(x,1) \tag{2.15}$$

where $x, y \in [0,1)$. Then our total vorticity in this domain must be zero:

$$\begin{aligned}\int_0^1\int_0^1 \omega\, dxdy &= \int_0^1\int_0^1 (-\frac{\partial u}{\partial y} + \frac{\partial v}{\partial x})\, dxdy \\ &= \int_0^1 -u\Big|_0^1 dx + \int_0^1 v\Big|_0^1 dy = 0\end{aligned} \tag{2.16}$$

We also set the integral of velocity be zero:

$$\int_0^1\int_0^1 \boldsymbol{u}\, dxdy = 0 \tag{2.17}$$

which means there is no potential flow (the flow without vorticity) in the domain, and our streamfunction ψ can be chosen to be periodic.

Now if the vorticity field $\omega(\boldsymbol{x})$ is given, theoretically we can get the velocity field $\boldsymbol{u}(\boldsymbol{x})$. First we can express $\omega(x,y)$ by its Fourier series:

$$\omega(x,y) = \sum_{\substack{n,m \\ n^2+m^2\neq 0}} \hat{\omega}(n,m)\exp\big(2\pi i(nx+my)\big) \tag{2.18}$$

Then by $\omega = -\Delta\psi$, we can get:

$$\psi(x,y) = \sum_{\substack{n,m \\ n^2+m^2\neq 0}} \frac{1}{4\pi(n^2+m^2)}\hat{\omega}(n,m)\exp\big(2\pi i(nx+my)\big) \tag{2.19}$$

Then by $\boldsymbol{u} = \nabla^{\perp}\psi$ we get the velocity field.

For point vortex system in periodic square, the vorticity field of point vortices could be written as:

$$\omega(\boldsymbol{x}) = \sum_{i=1}^{N} \Gamma_i \delta(\boldsymbol{x} - \boldsymbol{x}_i) \tag{2.20}$$

Then the Fourier coefficients are:

$$\hat{\omega}(n,m) = \int_0^1 \int_0^1 \omega(x,y)\exp\big(-2\pi i(nx+my)\big)\,dxdy \tag{2.21}$$

$$= \sum_{i=1}^{N} \Gamma_i \exp\big(-2\pi i(nx_i+my_i)\big) \tag{2.22}$$

Now by equation (2.19), we can get that:

$$\psi(x,y) = \sum_{\substack{n,m \\ n^2+m^2\neq 0}} \frac{1}{4\pi(n^2+m^2)}\Big(\sum_{i=1}^{N}\Gamma_i \exp\big(-2\pi i(nx_i+my_i)\big)\Big)\exp\big(2\pi i(nx+my)\big) \tag{2.23}$$

$$= \sum_{\substack{n,m \\ n^2+m^2\neq 0}} \sum_{i=1}^{N} \frac{\Gamma_i}{4\pi(n^2+m^2)}\exp\Big(2\pi i\big(n(x-x_i)+m(y-y_i)\big)\Big) \tag{2.24}$$

Then by $\boldsymbol{u} = \nabla^{\perp}\psi$ we get the velocity field. This velocity may diverge near each point vortex (x_i, y_i), so when we calculate the velocity of each point vortex, we should remove the self-generated velocity term. This means, when we do the summation of $\sum_{i=1}^{N}$, we should remove $i = j$ when we calculate $\boldsymbol{u}(x_j, y_j)$.

With the above analysis, we can define the Hamiltonian of the point vortex system

in periodic square:

$$\mathcal{H} = \sum_{\substack{n,m \\ n^2+m^2\neq 0}} \sum_{i<j}^{N} \frac{\Gamma_i \Gamma_j}{4\pi(n^2+m^2)} \exp\Big(2\pi i\big(n(x_i-x_j)+m(y_i-y_j)\big)\Big) \tag{2.25}$$

This Hamiltonian governs the evolution of our point vortex system also by:

$$\Gamma_i \frac{dx_i}{dt} = \frac{\partial \mathcal{H}}{\partial y_i} \tag{2.26}$$

$$\Gamma_i \frac{dy_i}{dt} = -\frac{\partial \mathcal{H}}{\partial x_i} \tag{2.27}$$

hence is also conserved during the evolution.

The physical meaning of this Hamiltonian is the energy of the system. If we compare equation (2.7) and (2.10), equation (2.24) and (2.25), we would find the Hamiltonian is close to the half of integral of stream function times vorticity:

$$\mathcal{H} \approx \frac{1}{2}\int \psi\omega \, dxdy \tag{2.28}$$

$$= \frac{1}{2}\int \psi(-\nabla^2\psi) \, dxdy \tag{2.29}$$

$$= \frac{1}{2}\int -\nabla\cdot(\psi\nabla\psi) + \nabla\psi\cdot\nabla\psi \, dxdy \tag{2.30}$$

$$= \frac{1}{2}\int -\nabla\cdot(\psi\nabla\psi) \, dxdy + \int \frac{1}{2}|\boldsymbol{u}|^2 \, dxdy \tag{2.31}$$

$$= \int \frac{1}{2}|\boldsymbol{u}|^2 \, dxdy \tag{2.32}$$

so this Hamiltonian kind of represent the kinetic energy of the flow field, even though for each point vortex, the energy is infinity if we integrate $\frac{1}{2}|\boldsymbol{u}|^2$ near it. Actually, when we calculate the Hamiltonian, we omit the self-generated energy of each point vortex, so the Hamiltonian will not be infinity.

2.3 Microcanonical ensemble of point vortices system

2.3.1 Microcanonical ensemble

In Onsager's 1949 paper, he used the microcanonical ensemble to analyze the point vortices system. Here we present some basic concepts of microcanonical ensemble.

For a system governed by Hamiltonian $\mathcal{H}(\mathbb{P}, \mathbb{Q})$, every point $(\mathbb{P}, \mathbb{Q})$ in its phase space cound be regard as a microstate of the system. The ensemble of the system could be regarded as a probability distribution of microstates, or a measure on its phase space $\rho(\mathbb{P}, \mathbb{Q})$ that satisfies:

$$\int \rho(\mathbb{P}, \mathbb{Q})\, d\mathbb{P} d\mathbb{Q} = 1 \tag{2.33}$$

If we have a property $O(\mathbb{P}, \mathbb{Q})$, then its average $\langle O \rangle$ can be measured by averaging $O(\mathbb{P}, \mathbb{Q})$ over all the possible microstate with its possibility:

$$\langle O \rangle = \int \rho(\mathbb{P}, \mathbb{Q})\, O(\mathbb{P}, \mathbb{Q})\, d\mathbb{P} d\mathbb{Q} \tag{2.34}$$

Microcanonical ensemble is used to describe an isolated system whose energy is conserved. In microcanonical ensemble we assume the ergodicity of the motion of the system. This assumption together with Liouville's theorem will bring us the following conclusion: every microstate at our fixed energy has the same probability. That is, if our system is at a fixed energy E_0, then the probability $\rho(\mathbb{P}, \mathbb{Q})$, satisfies:

$$\rho(\mathbb{P}, \mathbb{Q}) = \begin{cases} Const. & \text{if } \mathcal{H}(\mathbb{P}, \mathbb{Q}) = E_0 \\ 0 & \text{if } H(\mathbb{P}, \mathbb{Q}) \neq E_0 \end{cases} \tag{2.35}$$

Thus we calculate the properties of our ensemble by averaging over states with energy of the states in a shell $(E, E + \delta E)$, taking the limit $\delta E \to 0$ (Fig 2.1). Define the function $\Omega(E)$ to be the **phase space volume** of this shell:

$$\Omega(E) = \lim_{\delta E \to 0^+} \frac{1}{\delta E} \int_{E < \mathcal{H}(\mathbb{P}, \mathbb{Q}) < E + \delta E} d\mathbb{P} d\mathbb{Q} \tag{2.36}$$

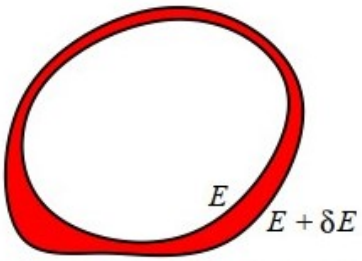

Figure 2.1: Enegy shell

The integral of $\Omega(E)$ over all the possible energy is the total volume of the phase space:

$$\int \Omega(E)\, dE = \int d\mathbb{P} d\mathbb{Q} = \text{Total volume of the phase space} \tag{2.37}$$

Now the probability $\rho(\mathbb{P}, \mathbb{Q})$ can be expressed by:

$$\rho(\mathbb{P}, \mathbb{Q}) = \frac{1}{\Omega(E_0)} \delta\big(E_0 - \mathcal{H}(\mathbb{P}, \mathbb{Q})\big) \tag{2.38}$$

The average property is:

$$\langle O \rangle = \int \rho(\mathbb{P}, \mathbb{Q})\, O(\mathbb{P}, \mathbb{Q})\, d\mathbb{P} d\mathbb{Q} = \int \frac{1}{\Omega(E_0)} \delta\big(E_0 - \mathcal{H}(\mathbb{P}, \mathbb{Q})\big)\, O(\mathbb{P}, \mathbb{Q})\, d\mathbb{P} d\mathbb{Q} \tag{2.39}$$

The phase space volume $\Omega(E)$ quantifies the number of microstates at a fixed energy E. In statistical mechanics, a key assumption is that every system tends to be in a macrostate that has more microstates. Following this idea, the entropy of microcanonical ensemble is defined by:

$$S(E) = \ln\big(\Omega(E)\big) \tag{2.40}$$

The temperature T is defined by:

$$\frac{1}{T} = \frac{dS}{dE} = \frac{\Omega'(E)}{\Omega(E)} \tag{2.41}$$

Usually the phase space volume $\Omega(E)$ is increasing with energy E, which makes the

temperature positive. However, in the folllowing we will see, for points vortex system in a confined domain, it is possible that $\Omega'(E) < 0$.

2.3.2 Negative temperature for point vortices system

For point vortex system in $\mathbb{R}^2$, recall the Hamiltonian:

$$\mathcal{H}(\boldsymbol{x}_1, \boldsymbol{x}_2, ..., \boldsymbol{x}_N) = -\frac{1}{2\pi} \sum_{i<j} \Gamma_i \Gamma_j \ln|\boldsymbol{x}_i - \boldsymbol{x}_j| \tag{2.42}$$

For $\boldsymbol{x}_i \in \mathbb{R}^2$, our physical picture of microcanonical ensemble is translation invariant: the point vortices have the same possibility to appear all over the $\mathbb{R}^2$ domain. Hence by definition (2.36), our phase space volume $\Omega(E)$ is infinity at any E, so we cannot calculate the temperature by (2.41).

For point vortices system on the periodic square, the Hamiltonian is:

$$\mathcal{H}(\boldsymbol{x}_1, \boldsymbol{x}_2, ..., \boldsymbol{x}_N) = \sum_{\substack{n,m \\ n^2+m^2 \neq 0}} \sum_{i<j}^{N} \frac{\Gamma_i \Gamma_j}{4\pi(n^2+m^2)} \exp\Big(2\pi i\big(n(x_i - x_j) + m(y_i - y_j)\big)\Big) \tag{2.43}$$

Denote $U = [0,1) \times [0,1)$ as our periodic square, then $\boldsymbol{x}_i \in U$. The measure of U is $1 < \infty$, so our total phase space volume is $1^N = 1 < \infty$. Hence:

$$\int_{-\infty}^{\infty} \Omega(E)\, dE = 1 < \infty \tag{2.44}$$

This tells us $\Omega(E) \to 0$ as $E \to \infty$ or $E \to -\infty$, so $\Omega'(E) < 0$ as $E \to \infty$. By this argument, Onsager concludes that when energy is high, we will have negative temperature for this system.

Montgomery and Joyce [9] proposed that by central limit theorem, as the number of point vortices $N \to \infty$, $\Omega(E)$ will approach a Gaussian:

$$\Omega(E) \xrightarrow{N\to\infty} \frac{1}{(2\pi B)^{1/2}} \exp(-\frac{(E-E_m)^2}{2B}) \tag{2.45}$$

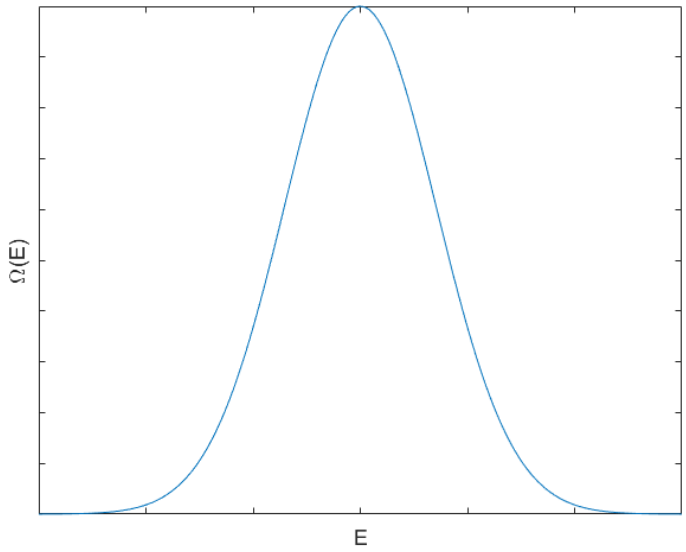

Figure 2.2: Schematic diagram of the phase space volume $\Omega(E)$ of point vortices system in a torus

See Figure 2.2. As E increases, $\Omega(E)$ first increases, reaches its maximum at a some energy E_m, then decreases to 0. The derivative $\Omega'(E)$ looks like Figure 2.3. The inverse temperature $\beta = \Omega'(E)/\Omega(E)$ looks like Figure 2.4, and the temperature $T = 1/\beta = \Omega(E)/\Omega'(E)$ looks like Figure 2.5. In the graph of temperature T, we observe that on the left side of $E = E_m$ the temperature is positive, and on the right side of $E = E_m$ the temperature is negative. The temperature will approach to 0^+ and 0^- respectively in $E \to -\infty$ and $E \to \infty$, and near the line $E = E_m$ the temperature is diverging to ∞.

2.4 The interpretation of negative temperature

In classical thermodynamics, temperature usually represents the average kinetic energy per particle of the thermodynamic system. If temperature is absolute zero, it means the system is frozen, and there is no motion of any particle. Hence, it is impossible for the system to have negative temperature.

However, the average kinetic energy theory cannot depict the essence of temperature. The second law of thermodynamics tells us that the balancing of temperature

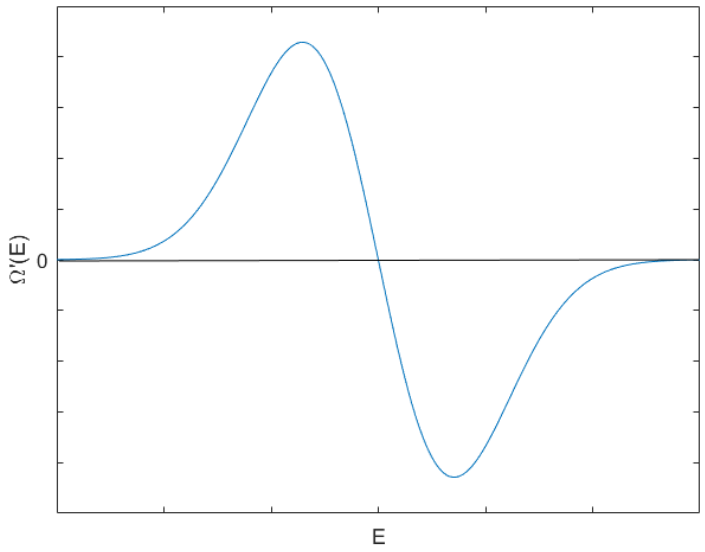

Figure 2.3: Schematic diagram of the derivative of phase space volume $\Omega'(E)$ of point vortices system in a torus

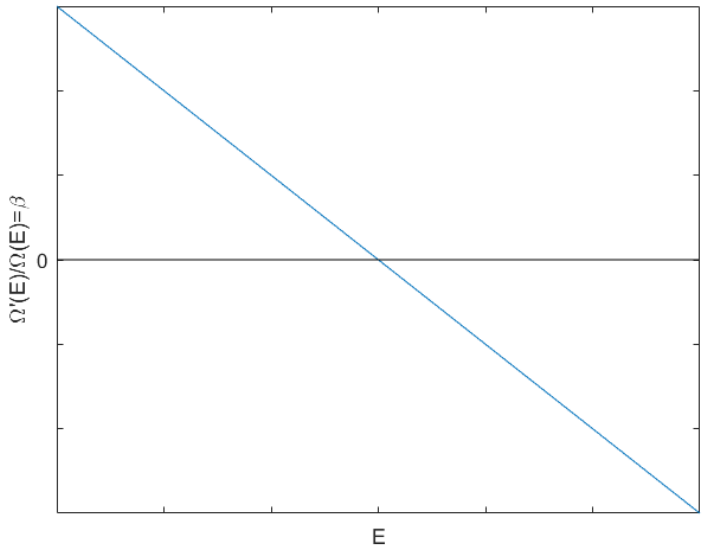

Figure 2.4: Schematic diagram of the inverse temperature $\beta = \Omega'(E)/\Omega(E)$ of point vortices system in a torus

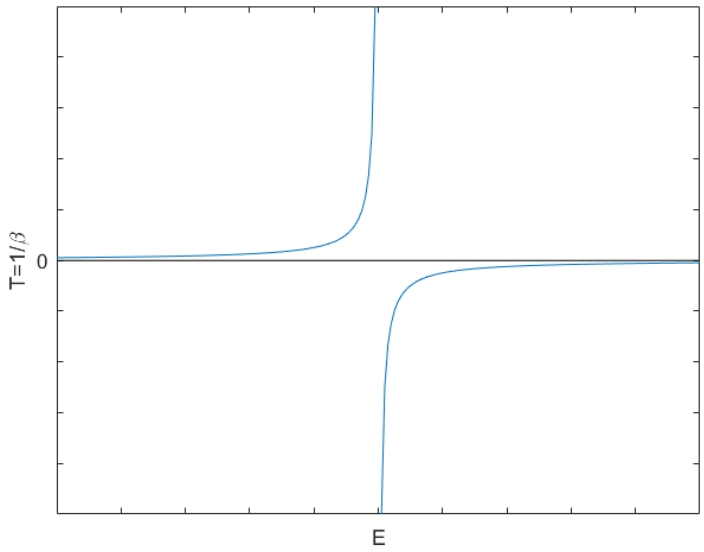

Figure 2.5: Schematic diagram of the temperature $T = 1/\beta = \Omega(E)/\Omega'(E)$ of point vortices system in a torus

is equal to the increase of entropy. The "increase of entropy" is a more general and fundamental understanding of the evolution direction of thermodynamic system. In statistical mechanics, usually we have a way to measure the entropy of the system, then based on this we cans calculate the temperature.

As defined in last section, for given entropy $S(E)$, we can define temperature by:

$$\frac{\partial S}{\partial E} = \frac{1}{T} \tag{2.46}$$

Hence, if a system has positive temperature, it means that the entropy will increase as the energy of the system grows. If a system has negative temperature, it means that the entropy will decrease as the energy of the system grows.

In a positive temperature system, if we have two regions (each region could be considered as a subsystem) that are in contact, with temperature T_1 and T_2 (say $T_1 > T_2 > 0$), then by the the law that entropy should increase, energy will tend to flow from high temperature region to low temperature region. The reason is as follows: suppose

we have a small amount of energy $\Delta E > 0$ flows from high temperature region to low temperature region, then the high temperature region will lose entropy by $\Delta S_1 = \frac{\Delta E}{T_1}$, and the low temperature region will gain entropy by $\Delta S_2 = \frac{\Delta E}{T_2}$, so the total entropy change of whole system is:

$$\Delta S_{total} = -\Delta S_1 + \Delta S_2 = -\frac{\Delta E}{T_1} + \frac{\Delta E}{T_2} = \Delta E \cdot \frac{T_1 - T_2}{T_1 T_2} > 0$$

since $T_1 > T_2$. Hence we conclude: for two systems with temperature $T_1 > T_2 > 0$, the energy tends to flow from system 1 to system 2.

We now consider the case of negative temperature. Suppose we have two systems with temperature $0 > T_1 > T_2$. Then to let:

$$-\Delta S_1 + \Delta S_2 = -\frac{\Delta E}{T_1} + \frac{\Delta E}{T_2} = \Delta E \cdot \frac{T_1 - T_2}{T_1 T_2} > 0$$

we must have $\Delta E > 0$, which means the energy tends to flow from system 1 to system 2.

Finally, we consider a system with positive temperature in contact with a system with negative temperature. Denote the temperature as $T_1 > 0 > T_2$, then if system 1 gains energy ΔE and system 2 loses energy ΔE, the total change of entropy is:

$$\Delta S_{total} = \frac{\Delta E}{T_1} - \frac{\Delta E}{T_2} > 0$$

so in this situation energy tends to flow from system 2 to system 1.

In summary, for two systems has different temperature T_1 and T_2, we have the following three laws:

- if $T_1 > T_2 > 0$, energy will tend to flow from system 1 to system 2;
- if $0 > T_1 > T_2$, energy will tend to flow from system 1 to system 2;
- if $T_1 > 0 > T_2$, energy will tend to flow from system 2 to system 1;

Chapter 3

Numerical method

3.1 Algorithm of the velocity of point vortex in periodic square

If we have N vortices in the domain $\mathbb{R}^2$, the velocity of the k-th vortex is generated by the remaining vortices, more precisely:

$$\mathbf{u}_k = -\frac{1}{2\pi} \sum_{\substack{i=1,\dots,N \\ i\neq k}} \Gamma_i \frac{(\mathbf{z}_k - \mathbf{z}_i)^\perp}{|\mathbf{z}_k - \mathbf{z}_i|^2} \tag{3.1}$$

Here, $\mathbf{z} = (x, y) \in \mathbb{R}^2$, $\mathbf{z}^\perp = (y, -x)$.

However, in periodic domain $[0, 1) \times [0, 1)$ we actually have infinite vortices in $\mathbb{R}^2$. We cannot summate them all in numerical simulation. It is natural to approximate as follows: for the vortices near the origin, we can use the above formula to sum the velocity they generate; for the vortices outsides some specific distance, one need to use some other way to approximate their effect.

Another way to calculate the velocity is using the partial derivative of the Hamiltonian for point vortex system in torus in chapter 2, but the summation in (2.25) is also hard to deal with. Here we choose to develop our algorithm basing on the equation (3.1).

3.1.1 The velocity generated by one cell

For periodic $[0,1)\times[0,1)$ domain in $\mathbb{R}^2$, denote $[i,i+1)\times[j,j+1)$ the (i,j)-th **cell**. First we want to quantify the velocity generated **by one cell**. Without loss of generality, suppose it's the $(0,0)$-th cell, since we can translate the position of cell to (i,j). Assume the vorticity field is known, and can be written as $\omega(x,y)=\sum_{k=1}^{n}\Gamma_k\delta(x-x_k,y-y_k)$, where $(x_k,y_k)\in[0,1)\times[0,1)$.

Suppose $|\mathbf{z_0}|=\sqrt{x_0^2+y_0^2}\gg 1$, the velocity generated by ω on point (x_0,y_0) is:

$$u_0^x=\frac{1}{2\pi}\int\frac{-(y_0-y)}{(x_0-x)^2+(y_0-y)^2}\omega(x,y)dxdy \tag{3.2}$$

$$u_0^y=\frac{1}{2\pi}\int\frac{x_0-x}{(x_0-x)^2+(y_0-y)^2}\omega(x,y)dxdy \tag{3.3}$$

Denote the moment of vorticity as:

$$M_{x^ny^m}=\int_0^1\int_0^1 x^ny^m\omega(x,y)dxdy \tag{3.4}$$

By our assumption: $M_{x^0y^0}=0$.

Now, to quantify the effect of every moment of vorticity, we write the Taylor expansion of the integrand function of equation (3.2) (3.3) in Table 3.1

Table 3.1: Taylor expansion of the integrand function of velocity.

$\frac{-(y_0-y)}{(x_0-x)^2+(y_0-y)^2}$ coefficient	$\frac{x_0-x}{(x_0-x)^2+(y_0-y)^2}$ coefficient	power
$-\frac{y_0}{x_0^2+y_0^2}$	$\frac{x_0}{x_0^2+y_0^2}$	1
$-\frac{2x_0y_0}{(x_0^2+y_0^2)^2}$	$\frac{x_0^2-y_0^2}{(x_0^2+y_0^2)^2}$	x

$\frac{x_0^2-y_0^2}{(x_0^2+y_0^2)^2}$	$\frac{2x_0y_0}{(x_0^2+y_0^2)^2}$	y
$\frac{y_0(-3x_0^2+y_0^2)}{(x_0^2+y_0^2)^3}$	$\frac{x_0(x_0^2-3y_0^2)}{(x_0^2+y_0^2)^3}$	x^2
$\frac{2x_0(x_0^2-3y_0^2)}{(x_0^2+y_0^2)^3}$	$\frac{2y_0(3x_0^2-y_0^2)}{(x_0^2+y_0^2)^3}$	xy
$-\frac{y_0(-3x_0^2+y_0^2)}{(x_0^2+y_0^2)^3}$	$-\frac{x_0(x_0^2-3y_0^2)}{(x_0^2+y_0^2)^3}$	y^2
$-\frac{4x_0y_0(x_0^2-y_0^2)}{(x_0^2+y_0^2)^3}$	$\frac{x_0^4-6y_0^2x_0^2+y_0^4}{(x_0^2+y_0^2)^4}$	x^3
$\frac{3(x_0^4-6x_0^2y_0^2+y_0^2)}{(x_0^2+y_0^2)^4}$	$\frac{12x_0y_0(x_0^2-y_0^2)}{(x_0^2+y_0^2)^4}$	x^2y
$\frac{12x_0y_0(x_0^2-y_0^2)}{(x_0^2+y_0^2)^4}$	$-\frac{3(x_0^4-6y_0^2x_0^2+y_0^4)}{(x_0^2+y_0^2)^4}$	xy^2
$\frac{-x_0^4+6x_0^2y_0^2-y_0^4}{(x_0^2+y_0^2)^4}$	$-\frac{4x_0y_0(x_0^2-y_0^2)}{(x_0^2+y_0^2)^4}$	y^3
$-\frac{y_0(-10x_0^2y_0^2+5x_0^4+y_0^4)}{(x_0^2+y_0^2)^5}$	$\frac{x_0(-10x_0^2y_0^2+x_0^4+5y_0^4)}{(x_0^2+y_0^2)^5}$	x^4
$\frac{4x_0(-10x_0^2y_0^2+x_0^4+5y_0^4)}{(x_0^2+y_0^2)^5}$	$\frac{4y_0(-10x_0^2y_0^2+5x_0^4+y_0^4)}{(x_0^2+y_0^2)^5}$	x^3y
$\frac{6y_0(-10x_0^2y_0^2+5x_0^4+y_0^4)}{(x_0^2+y_0^2)^5}$	$-\frac{6x_0(-10x_0^2y_0^2+x_0^4+5y_0^4)}{(x_0^2+y_0^2)^5}$	x^2y^2
$-\frac{4x_0(-10x_0^2y_0^2+x_0^4+5y_0^4)}{(x_0^2+y_0^2)^5}$	$-\frac{4y_0(-10x_0^2y_0^2+5x_0^4+y_0^4)}{(x_0^2+y_0^2)^5}$	xy^3
$-\frac{y_0(-10x_0^2y_0^2+5x_0^4+y_0^4)}{(x_0^2+y_0^2)^5}$	$\frac{x_0(-10x_0^2y_0^2+x_0^4+5y_0^4)}{(x_0^2+y_0^2)^5}$	y^4
...	...	...

From the above Taylor expansion, the velocity on point (x_0, y_0) generated by $(0, 0)$-th

cell is:

$$2\pi u_0^x = -\frac{2x_0y_0}{(x_0^2+y_0^2)^2}M_x + \frac{x_0^2-y_0^2}{(x_0^2+y_0^2)^2}M_y + \frac{y_0(-3x_0^2+y_0^2)}{(x_0^2+y_0^2)^3}M_{x^2} + \frac{2x_0(x_0^2-3y_0^2)}{(x_0^2+y_0^2)^3}M_{xy} - \frac{y_0(-3x_0^2+y_0^2)}{(x_0^2+y_0^2)^3}M_{y^2} + ... \tag{3.5}$$

$$2\pi u_0^y = \frac{x_0^2-y_0^2}{(x_0^2+y_0^2)^2}M_x + \frac{2x_0y_0}{(x_0^2+y_0^2)^2}M_y + \frac{x_0(x_0^2-3y_0^2)}{(x_0^2+y_0^2)^3}M_{x^2} + \frac{2y_0(3x_0^2-y_0^2)}{(x_0^2+y_0^2)^3}M_{xy} - \frac{x_0(x_0^2-3y_0^2)}{(x_0^2+y_0^2)^3}M_{y^2} + ... \tag{3.6}$$

By changing of variables, the velocity on point (x, y) generated by the (i, j)th cell is:

$$2\pi u^x = -\frac{2(x-i)(y-j)}{((x-i)^2+(y-j)^2)^2}M_x + \frac{(x-i)^2-(y-j)^2}{((x-i)^2+(y-j)^2)^2}M_y + \frac{(y-j)(-3(x-i)^2+(y-j)^2)}{((x-i)^2+(y-j)^2)^3}M_{x^2} + \frac{2(x-i)((x-i)^2-3(y-j)^2)}{((x-i)^2+(y-j)^2)^3}M_{xy} - \frac{(y-j)(-3(x-i)^2+(y-j)^2)}{((x-i)^2+(y-j)^2)^3}M_{y^2} + ... \tag{3.7}$$

$$2\pi u^y = \frac{(x-i)^2-(y-j)^2}{((x-i)^2+(y-j)^2)^2}M_x + \frac{2(x-i)(y-j)}{((x-i)^2+(y-j)^2)^2}M_y + \frac{(x-i)((x-i)^2-3(y-j)^2)}{((x-i)^2+(y-j)^2)^3}M_{x^2} + \frac{2(y-j)(3(x-i)^2-(y-j)^2)}{((x-i)^2+(y-j)^2)^3}M_{xy} - \frac{(x-i)((x-i)^2-3(y-j)^2)}{((x-i)^2+(y-j)^2)^3}M_{y^2} + ... \tag{3.8}$$

For detailed expansion see the Table 3.2.

Table 3.2: Velocity on point (x, y) generated by the (i, j)th cell

u_x	u_y	moment
$-\frac{2(x-i)(y-j)}{((x-i)^2+(y-j)^2)^2}$	$\frac{(x-i)^2-(y-j)^2}{((x-i)^2+(y-j)^2)^2}$	M_x

$\frac{(x-i)^2-(y-j)^2}{((x-i)^2+(y-j)^2)^2}$	$\frac{2(x-i)(y-j)}{((x-i)^2+(y-j)^2)^2}$	M_y
$\frac{(y-j)(-3(x-i)^2+(y-j)^2)}{((x-i)^2+(y-j)^2)^3}$	$\frac{(x-i)((x-i)^2-3(y-j)^2)}{((x-i)^2+(y-j)^2)^3}$	M_{x^2}
$\frac{2(x-i)((x-i)^2-3(y-j)^2)}{((x-i)^2+(y-j)^2)^3}$	$\frac{2(y-j)(3(x-i)^2-(y-j)^2)}{((x-i)^2+(y-j)^2)^3}$	M_{xy}
$-\frac{(y-j)(-3(x-i)^2+(y-j)^2)}{((x-i)^2+(y-j)^2)^3}$	$-\frac{(x-i)((x-i)^2-3(y-j)^2)}{((x-i)^2+(y-j)^2)^3}$	M_{y^2}
$-\frac{4(x-i)(y-j)((x-i)^2-(y-j)^2)}{((x-i)^2+(y-j)^2)^4}$	$\frac{(x-i)^4-6(y-j)^2(x-i)^2+(y-j)^4}{((x-i)^2+(y-j)^2)^4}$	M_{x^3}
$\frac{3((x-i)^4-6(x-i)^2(y-j)^2+(y-j)^2)}{((x-i)^2+(y-j)^2)^4}$	$\frac{12(x-i)(y-j)((x-i)^2-(y-j)^2)}{((x-i)^2+(y-j)^2)^4}$	M_{x^2y}
$\frac{12(x-i)(y-j)((x-i)^2-(y-j)^2)}{((x-i)^2+(y-j)^2)^4}$	$-\frac{3((x-i)^4-6(y-j)^2(x-i)^2+(y-j)^4)}{((x-i)^2+(y-j)^2)^4}$	M_{xy^2}
$\frac{-(x-i)^4+6(x-i)^2(y-j)^2-(y-j)^4}{((x-i)^2+(y-j)^2)^4}$	$-\frac{4(x-i)(y-j)((x-i)^2-(y-j)^2)}{((x-i)^2+(y-j)^2)^4}$	M_{y^3}
$-\frac{(y-j)(-10(x-i)^2(y-j)^2+5(x-i)^4+(y-j)^4)}{((x-i)^2+(y-j)^2)^5}$	$\frac{(x-i)(-10(x-i)^2(y-j)^2+(x-i)^4+5(y-j)^4)}{((x-i)^2+(y-j)^2)^5}$	M_{x^4}
$\frac{4(x-i)(-10(x-i)^2(y-j)^2+(x-i)^4+5(y-j)^4)}{((x-i)^2+(y-j)^2)^5}$	$\frac{4(y-j)(-10(x-i)^2(y-j)^2+5(x-i)^4+(y-j)^4)}{((x-i)^2+(y-j)^2)^5}$	M_{x^3y}
$\frac{6(y-j)(-10(x-i)^2(y-j)^2+5(x-i)^4+(y-j)^4)}{((x-i)^2+(y-j)^2)^5}$	$-\frac{6(x-i)(-10(x-i)^2(y-j)^2+(x-i)^4+5(y-j)^4)}{((x-i)^2+(y-j)^2)^5}$	$M_{x^2y^2}$
$-\frac{4(x-i)(-10(x-i)^2(y-j)^2+(x-i)^4+5(y-j)^4)}{((x-i)^2+(y-j)^2)^5}$	$-\frac{4(y-j)(-10(x-i)^2(y-j)^2+5(x-i)^4+(y-j)^4)}{((x-i)^2+(y-j)^2)^5}$	M_{xy^3}
$-\frac{(y-j)(-10(x-i)^2(y-j)^2+5(x-i)^4+(y-j)^4)}{((x-i)^2+(y-j)^2)^5}$	$\frac{(x-i)(-10(x-i)^2(y-j)^2+(x-i)^4+5(y-j)^4)}{((x-i)^2+(y-j)^2)^5}$	M_{y^4}
...	...	...

3.1.2 Summation of the velocity generated by cells

As mentioned in the overview, for the velocity generated by cells close to origin, we can use formula (3.1). For the velocity generated by the unlimited cells far away to the origin, we need to sum them together and control the accuracy.

Without loss of generality, we fix an integer $K \gg 1$. For the (i,j)-th cell with $|i| \le K$, $|j| \le K$, we call it an **inner cell**. For a cell that is not inner cell we call it an **outer cell**.

The velocity generated by all the outer cells on point $(x,y) \in (0,1) \times (0,1)$ is:

$$\begin{aligned}
2\pi u^x_{out} = \sum_{\substack{|i|>K \\ \text{or } |j|>K}} \Bigg(& -\frac{2(x-i)(y-j)}{((x-i)^2+(y-j)^2)^2} M_x + \frac{(x-i)^2-(y-j)^2}{((x-i)^2+(y-j)^2)^2} M_y \\
& + \frac{(y-j)(-3(x-i)^2+(y-j)^2)}{((x-i)^2+(y-j)^2)^3} M_{x^2} + \frac{2(x-i)((x-i)^2-3(y-j)^2)}{((x-i)^2+(y-j)^2)^3} M_{xy} \\
& - \frac{(y-j)(-3(x-i)^2+(y-j)^2)}{((x-i)^2+(y-j)^2)^3} M_{y^2} + ... \\
& - \frac{(y-j)(-10(x-i)^2(y-j)^2+5(x-i)^4+(y-j)^4)}{((x-i)^2+(y-j)^2)^5} M_{y^4} \Bigg) + O(\frac{1}{K^4}) \qquad (3.9) \\
2\pi u^y_{out} = \sum_{\substack{|i|>K \\ \text{or } |j|>K}} \Bigg(& \frac{(x-i)^2-(y-j)^2}{((x-i)^2+(y-j)^2)^2} M_x + \frac{2(x-i)(y-j)}{((x-i)^2+(y-j)^2)^2} M_y \\
& + \frac{(x-i)((x-i)^2-3(y-j)^2)}{((x-i)^2+(y-j)^2)^3} M_{x^2} + \frac{2(y-j)(3(x-i)^2-(y-j)^2)}{((x-i)^2+(y-j)^2)^3} M_{xy} \\
& - \frac{(x-i)((x-i)^2-3(y-j)^2)}{((x-i)^2+(y-j)^2)^3} M_{y^2} + ... \\
& + \frac{(x-i)(-10(x-i)^2(y-j)^2+(x-i)^4+5(y-j)^4)}{((x-i)^2+(y-j)^2)^5} M_{y^4} \Bigg) + O(\frac{1}{K^4}) \qquad (3.10)
\end{aligned}$$

Here the truncation error is $O(\frac{1}{K^4})$, because for moment $M_{x^n y^m}$ where $m+n \ge 5$, the coefficient before them is at least in the order of:

$$\sum_{\substack{|i|>K \\ \text{or } |j|>K}} \frac{1}{(\sqrt{i^2+j^2})^6} \sim \int_{\sqrt{x^2+y^2}>K} \frac{1}{(\sqrt{x^2+y^2})^6} dxdy \sim \int_K^\infty \frac{1}{r^6} 2\pi r dr \sim \frac{1}{K^4} \qquad (3.11)$$

In addition, for all the cases in the thesis, we would always keep the summation of the

strength of positive (or negative) point vortices be 1:

$$\sum_{\Gamma_i>0} \Gamma_i = \sum_{\Gamma_i<0} |\Gamma_i| = 1 \tag{3.12}$$

Hence all the moment of vorticity $M_{x^n y^m} = \int_0^1 \int_0^1 x^n y^m \omega(x,y) dxdy$ is less than 1.

For the terms inside the summation in equation (3.9) (3.10), we write their Taylor expansions till the magnitude of $\frac{1}{K^5}$. The details are in the **Appendix A**. For Taylor series greater than $\frac{1}{K^5}$, the above analysis tells us the summation will be in the order of $O(\frac{1}{K^4})$, which is within our truncation error.

Then we take the summation of the remaining terms, and it turns out that most of them disappear after summation (see **Appendix A**). We finally get a simplified expression of u^x_{out} and u^y_{out}:

$$u^x_{out} = \frac{C_K}{2\pi}\left[6xyM_x + 3(x^2-y^2)M_y - 3yM_{x^2} - 6xM_{xy} + 3yM_{y^2} + 3M_{x^2y} - M_{y^3}\right] + O(\frac{1}{K^4}) \tag{3.13}$$

$$u^y_{out} = \frac{C_K}{2\pi}\left[3(x^2-y^2)M_x - 6xyM_y - 3xM_{x^2} + 6yM_{xy} + 3xM_{y^2} + M_{x^3} - 3M_{xy^2}\right] + O(\frac{1}{K^4}) \tag{3.14}$$

where $C_K = \sum_{\substack{|i|>K \\ \text{or } |j|>K}} \frac{(i^4-6i^2j^2+j^4)}{(i^2+j^2)^4} = 3.15121 - \sum_{\substack{|i|\le K \\ |j|\le K}} \frac{(i^4-6i^2j^2+j^4)}{(i^2+j^2)^4}$

By formula (3.1), we can get the velocity (u^x_{in}, u^y_{in}) generated by inner cell with no truncation error. Hence the total velocity of position $(x,y) \in [0,1) \times [0,1)$ is:

$$u^x = u^x_{in} + u^x_{out} \tag{3.15}$$

$$u^y = u^y_{in} + u^x_{out} \tag{3.16}$$

To choose the proper K, we can do some dimensional analysis. Our length scale is $L = 1$, and our vorticity scale is $\Gamma = 1$ (because the total same sign vorticity is 1), so our velocity scale is $U = L \times \Gamma = 1$. If we set $K = 5$, then the velocity field has error $O(\frac{1}{5^4}) \sim 1 \times 10^{-3} \ll 1$. Hence $K = 5$ might be a good choice.

We can also estimate the real velocity magnitude by doing an experience: we randomly set 2000 point vortices in the domain, with half of them in the strength of 0.001 and half -0.001. By calculating their velocity using $K = 5$, we find their average velocity is about 0.04, which is 40 times the velocity error.

Later we will see, for randomly distributed vortices, the velocity is much smaller than the velocity of distribution with coalescence of same sign vortices or dipoles (a pair of different sign vortices). In this case the vorticity is too evenly distributed. Hence, if in this case $K = 5$ is proper, then $K = 5$ should be proper in other cases.

In the rest of the thesis, if there is no special statement, we are using $K = 5$.

3.2 Time advancement

For time advancement, the most intuitive method is the **Euler method**. Since we know the expression of velocity, we can set:

$$\mathbf{x}(t + \Delta t) = \mathbf{x}(t) + \mathbf{u}(\mathbf{x}(t))\Delta t \tag{3.17}$$

However, the main term of truncation error of Euler method is: $\frac{u'(t)}{2}\Delta t^2 \sim O(\Delta t^2)$, which is too rough for our purposes. Instead, we would like to use the following **predictor–corrector method**:

$$\mathbf{x}^*(t + \Delta t) = \mathbf{x}(t) + \mathbf{u}(\mathbf{x}(t))\Delta t \tag{3.18}$$

$$\mathbf{x}(t + \Delta t) = \mathbf{x}(t) + \frac{1}{2}\big[\mathbf{u}(\mathbf{x}(t)) + \mathbf{u}(\mathbf{x}^*(t + \Delta t))\big] \tag{3.19}$$

The truncation error of this method is $O(\Delta t^3)$.

To choose a proper number of Δt, we consider the following case.

Suppose there are two vortices with the same sign $\Gamma_1 = \Gamma_2 = \Gamma = 1$ in $\mathbb{R}^2$, then the two vortices will move in a circle with velocity:

$$u = \frac{\Gamma}{2\pi d}$$

where d is their distance and diameter of the circle.

In simulation, after one time advancement Δt, the vortex will move around the center of circle with angle:

$$\Delta\theta = \frac{2u\Delta t}{d} = \frac{\Gamma\Delta t}{\pi d^2} \tag{3.20}$$

If our $\Delta t = 1 \times 10^{-4}$, then for $d = 1 \times 10^{-2}$, the change of angle $\Delta\theta$ will be in the order of 0.3. As d get smaller, $\Delta\theta$ will get too big that our predictor–corrector method may totally lose accuracy. We can run this case with several Δt and initial distance d, and see the change of their distance, in Table 3.3

Δt	t	change of distance
1×10^{-3}	1	$0.01 \to 0.0302$
1×10^{-4}	0.1	$0.01 \to 0.0107$
1×10^{-4}	0.1	$0.001 \to 0.0164$
1×10^{-4}	1	$0.01 \to 0.0129$

Table 3.3: Change of distance between two equal vortices rotate in a circle

In the first and third lines of Table 3.3, the distance changed too much after running for only 1000 time step, which means under $\Delta t = 1 \times 10^{-3}$, the smallest distance we can capture is about 0.03, while under $\Delta t = 1 \times 10^{-4}$, the smallest distance we can capture is about 0.01. The smallest distance d we can capture is in the order of $\sqrt{\Delta t}$, which is consistent with equation (3.20).

Since our domain is $[0, 1) \times [0, 1)$, we would like the smallest distance of two same

sign vortices be about 0.003. By the above analysis, we can set our Δt be:

$$\Delta t \sim 0.003^2/\Gamma \sim 10^{-5}/\Gamma \tag{3.21}$$

To elaborate the above equation, suppose we have 2000 point vortices in the domain, with half in the strength 0.001 and half -0.001, then the Δt would be:

$$\Delta t = 10^{-5}/0.001 = 10^{-2}$$

Since we always set the total same sign vorticity to be $\Gamma = 1$, and the scale of our domain is $L = 1$, by dimensional analysis, this dimensionless time represents the **large eddy turn over time**. The physical meaning of this dimensionless time is as follows: during one dimensionless time, the largest eddy will spin over the whole domain by one circle. For cases in this thesis, we usually run the case over 100 large eddy turn over time, which is commonly accepted as a long time.

Chapter 4

Simulation results

4.1 Infinity temperature

If we randomly set up the position of the N ($N \gg 1$) point vortices in the domain, our simulation shows that it tends to stay random as time goes by.

4.1.1 Case 1: randomly distributed point vortices in a torus

In Figure 4.1, we randomly set 2000 point vortices in the 2D periodic domain, with half in the strength of 0.001 and half -0.001. We let this system developing for 100 dimensionless time, and the distribution (Figure 4.1) looks still quite random.

It might be confusing that no large structure appears in this case. Recall for 2D turbulence, energy generically flows to large scale, so we expect to see large scale vortices as time goes by. It seems to suggest that, to initiate the formation of large vortices, there should be some small scales of vortices to begin with. This will be explained more in the next case (negative temperature case).

4.1.2 Phase space analysis

Randomly setting point vortices in the torus domain is equivalent to randomly picking up a point in the phase space, which means randomly picking up a point in the area under the curve $\Omega(E)$ in Figure 2.2. Since this distribution cannot form large structure of vortices (which should look like Figure 4.2), which Onsager claims to have negative

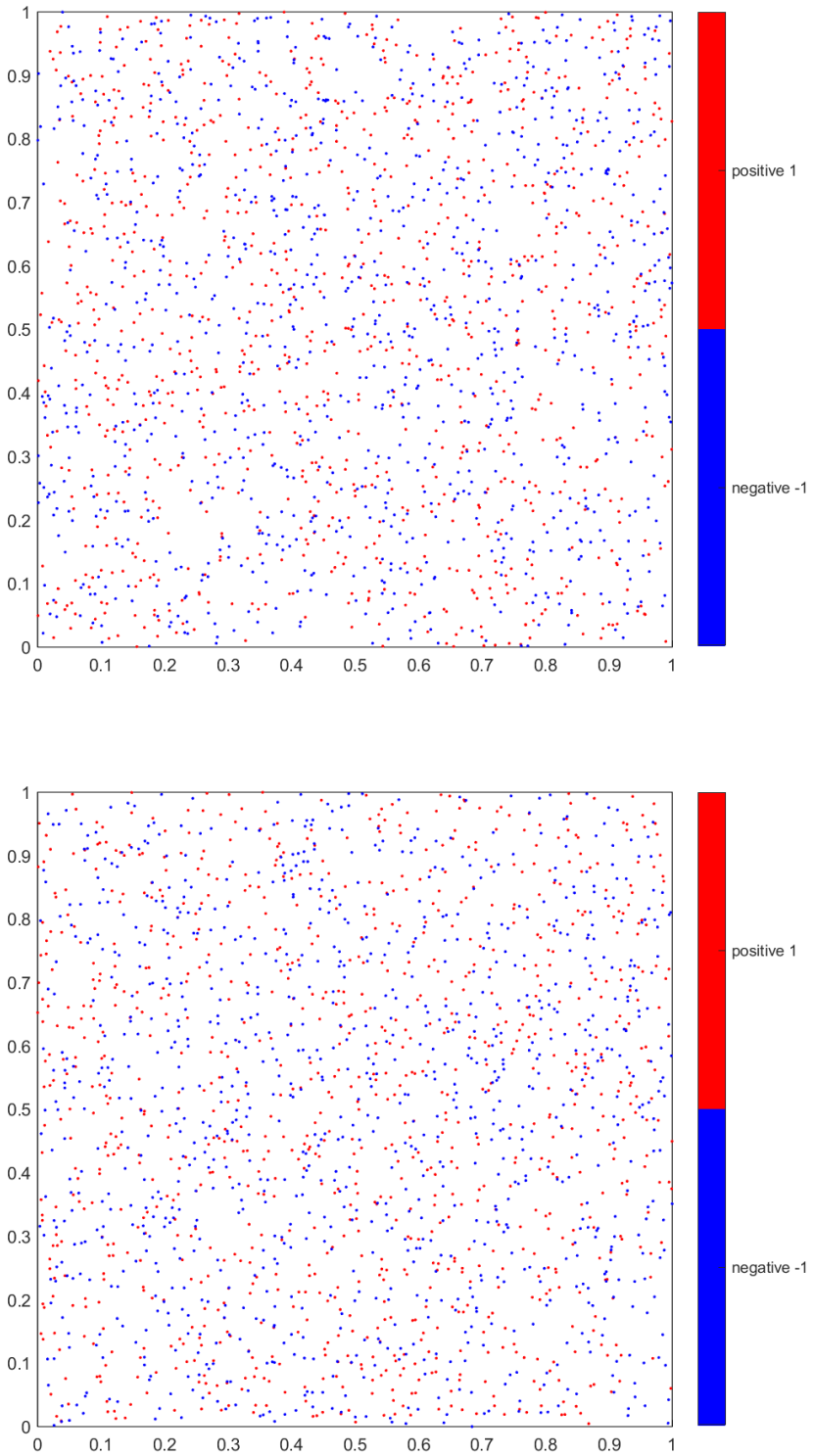

Figure 4.1: Randomly distributed 2000 vortices in a torus; after developing for 100 dimensionless time

temperature, we conclude that it is almost impossible to find a case with negative temperature by randomly picking up a point in the phase space. This means, the case with negative temperature occupies very little volume of the phase space.

Instead, this randomly distributed vortices occupied almost all the phase space (the area under $\Omega(E)$). We call this kind of distribution has "**infinity temperature**". The terminology is suggested from the heuristic that this random distribution is a random point near the line $E = E_m$ in the graph of $\Omega(E)$ (Figure 2.2), and near the line $E = E_m$ the temperature T approaches ∞ (Figure 2.5). Later we will see in the negative temperature region and positive temperature region, the system will have different properties than this kind of distribution. The interactions (interchanges of energy and entropy) between different temperature regions approximately satisfy the classical point of view of temperature.

4.2 Negative temperature

In Figure 2.5 we know for energy E large enough, we may have negative temperature. In 2D periodic domain, this energy is:

$$E = \mathcal{H}(\boldsymbol{x}_1, \boldsymbol{x}_2, ..., \boldsymbol{x}_N) = \sum_{i<j} \sum_{\boldsymbol{n}} \frac{\Gamma_i \Gamma_j}{4\pi^2 |\boldsymbol{n}|^2} \exp\big(2\pi i \boldsymbol{n} \cdot (\boldsymbol{x}_i - \boldsymbol{x}_j)\big), \quad \boldsymbol{n} \in \mathbb{Z}^2, \boldsymbol{n} \neq (0,0) \tag{4.1}$$

From this expression, if we look at the dominant term $|\boldsymbol{n}| = 1$, we can observe that for two same sign vortices ($\Gamma_i \Gamma_j > 0$), the closer they are, the larger energy they may have. Also, if we look at the Hamiltonian of vortices system in $\mathbb{R}^2$:

$$\mathcal{H}(\boldsymbol{x}_1, \boldsymbol{x}_2, ..., \boldsymbol{x}_N) = \sum_{i<j} -\frac{\Gamma_i \Gamma_j}{2\pi} \log(|\boldsymbol{x}_i - \boldsymbol{x}_j|) \tag{4.2}$$

we may also conclude that we can let two same sign vortices be very close to each other to make $\mathcal{H}$ sufficiently large.

Hence, to create a distribution with negative temperature, it suffices to cluster the same sigh vortices.

4.2.1 Case 2: two opposite sign vortex patches will never merge

An obvious case is clustering all the positive vortices and all the negative vortices, see Figure 4.2. We set 1000 positive point vortices (strength 0.001) and 1000 point negative vortices (strength -0.001) separately inside two big circles. After a long time (100 dimensionless time), the two big vortex patches are still present, not mixing together.

4.2.2 The energy difference between case 1 and case 2

As mentioned before, clustering of same sign point vortices will make the energy (Hamiltonian) increase, so the energy of the randomly distributed point vortex system (Figure 4.1) is much smaller than the energy of the same sign clustered point vortex system (Figure 4.2). Now let us estimate the energy of these two systems by using Equation (4.2). Assume the area of our domain is V; the number of point vortices is N (with $N/2$ positive vortices and $N/2$ negative vortices all with unit magnitude).

For the first randomly distributed case, every positive point vortex (assume its position is $\boldsymbol{x}_i^+$) has $(N/2-1)$ positive point vortices and $N/2$ negative point vortices evenly distributed near it. Hence the summation of the interaction term of this point vortex with other point vortices is:

$$\mathcal{H}_i^+ = \sum_{j=1\ldots N/2, j\neq i} -\frac{1}{2\pi}\log(|\boldsymbol{x}_i^+ - \boldsymbol{x}_j^+|) + \sum_{j=1\ldots N/2} \frac{1}{2\pi}\log(|\boldsymbol{x}_i^+ - \boldsymbol{x}_j^-|)$$

For every $\boldsymbol{x}_j^+$, we can find a $\boldsymbol{x}_j^- \approx \boldsymbol{x}_j^+$ s.t.

$$-\frac{1}{2\pi}\log(|\boldsymbol{x}_i^+ - \boldsymbol{x}_j^+|) + \frac{1}{2\pi}\log(|\boldsymbol{x}_i^+ - \boldsymbol{x}_j^-|) \approx 0$$

Hence, this summation can be approximated by the interaction of $\boldsymbol{x}_i^+$ with one of the $\boldsymbol{x}_j^-$ that has an averaged distance to $\boldsymbol{x}_i^+$. Since the domain's area is V, we could let this averaged distance be $\sqrt{V}$, so:

$$\mathcal{H}_i^+ \approx \frac{1}{2\pi}\log(\sqrt{V})$$

Similarly analysis, we can get that $\mathcal{H}_i^- \approx \frac{1}{2\pi}\log(\sqrt{V})$. Hence the total energy of this

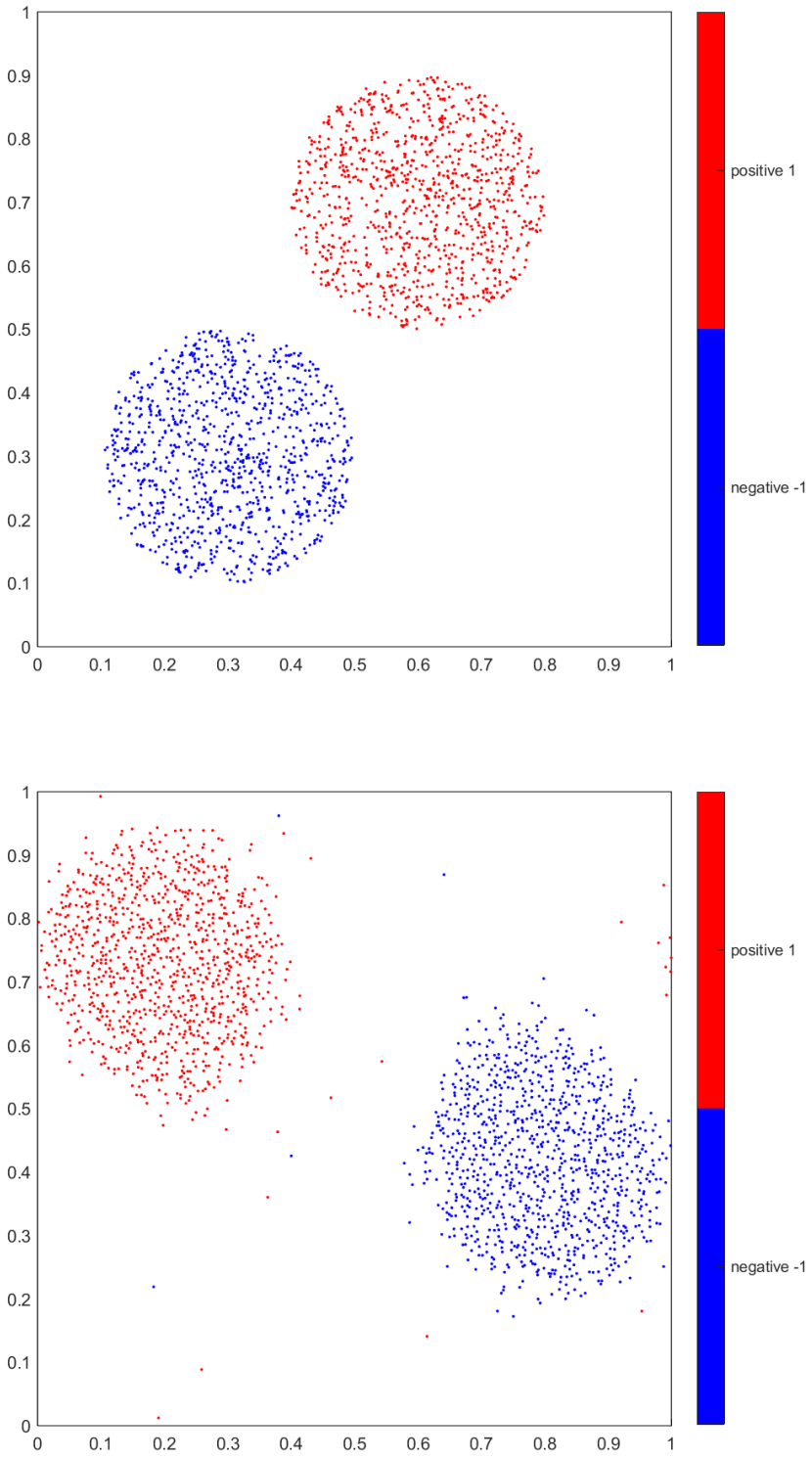

Figure 4.2: 2000 vortices, with same sign vortices clustered in a circle; after developing for 100 dimensionless time

case is:

$$\mathcal{H}_{random} = \frac{1}{2}\sum_{i=1}^{N/2}(\mathcal{H}_i^+ + \mathcal{H}_i^-) \approx \frac{N}{4\pi}\log(\sqrt{V}) \tag{4.3}$$

For the same sign clustered case, assume the radius of the circle is $r < \sqrt{V}$, and the distance of two circle is $d > 2r$ ($d < \sqrt{V}$), then the summation of the interaction term of one random positive point vortex with other point vortices is:

$$\begin{aligned}\mathcal{H}_i^+ &= \sum_{j=1\ldots N/2, j\neq i} -\frac{1}{2\pi}\log(|\boldsymbol{x}_i^+ - \boldsymbol{x}_j^+|) + \sum_{j=1\ldots N/2}\frac{1}{2\pi}\log(|\boldsymbol{x}_i^+ - \boldsymbol{x}_j^-|)\\ &\approx (\frac{N}{2}-1)(-\frac{1}{2\pi})\log(r) + \frac{N}{2}\frac{1}{2\pi}\log(d)\\ &= \frac{1}{2\pi}\log(r) + \frac{N}{4\pi}\log(\frac{d}{r})\end{aligned}$$

Similarly analysis, we can get that $\mathcal{H}_i^- \approx \mathcal{H}_i^+$. Hence the total energy of this case is:

$$\mathcal{H}_{cluster} = \frac{1}{2}\sum_{i=1}^{N/2}(\mathcal{H}_i^+ + \mathcal{H}_i^-) \approx \frac{N}{4\pi}\log(r) + \frac{N^2}{8\pi}\log(\frac{d}{r})$$

Hence, the energy difference of the two system is:

$$\Delta E = \mathcal{H}_{cluster} - \mathcal{H}_{random} \approx \frac{N^2}{8\pi}\log(\frac{d}{r}) - \frac{N}{4\pi}\log(\frac{\sqrt{V}}{r})$$

Since $d \sim \sqrt{V}$, and $N \gg 0$, so the first term $\frac{N^2}{8\pi}\log(\frac{d}{r})$ must be much greater than the second term $\frac{N}{4\pi}\log(\frac{\sqrt{V}}{r})$. Hence we have $\Delta E > 0$.

The evolution of point vortex system is an energy conserved process, so it is impossible for the former distribution to evolve to the vortices clustering distribution. This may help us to understand the confusion of last section.

4.2.3 Case 3: 2D turbulence

The main purpose of this article is to study the merging of small vortices in 2D domain, and here by this case we will show that point vortex system can capture such phenomenon.

In Figure 4.3, we set 2000 point vortices in a unit torus, with half in strength of 0.001

and half -0.001. We let every 20 same sign point vortices clustering in a small circle with radius 0.01, so we have 100 small vortex patches. Then let these 100 vortex patches randomly distributed in the domain. After the system developing for 200 dimensionless time, we find there are only 2 big vortex patches in the domain 4.3, while the rest of the domain is filled with randomly distributed different sign vortices.

In numerical simulation, we find such a distribution— two recognizable big vortex patches with different sign, and the rest of the domain randomly filled with different sign vortices— will last for a long time. This phenominon is pretty similar to case 2, where we found that two vortex patches will never merge. By estimating the energy of the system, we can find the energy this case is also much greater than the energy of the randomly distributed case, so by energy conservation it cannot evolute to the randomly distributed case. This may explain that the two recognizable big vortex patches will never merge or disappear to the background— it contains the energy of the system.

4.2.4 Coexistence of negative and infinity temperature

Since case 3 has high energy, by Figure 2.5 this system has negative temperature. Meanwhile, we observe that in the final distribution, most of the domain is filled with the randomly distributed point vortices, which is very similar to the infinity temperature case. Now we are going to show this system can be seperated into two subsystems, with one in negative temperature and another in infinity temperature.

For the final distribution, denote the index of point vortices that form the large vortex patches as $i \in U$ (keep the total vorticity be zero), the index of point vortices that are in the randomly distributed different sign vortices background as $i \in V$, then the energy of the system could be seperated into three parts:

$$\mathcal{H} = \mathcal{H}_U + \mathcal{H}_V + \mathcal{H}_{U,V} \tag{4.4}$$

The first term is the self-energy of point vortex system for vortices in U; the second term is the self-energy of point vortex system for vortices in V; the third term is the interaction energy between vortices in U and vortices in V. By equation (4.1), the term

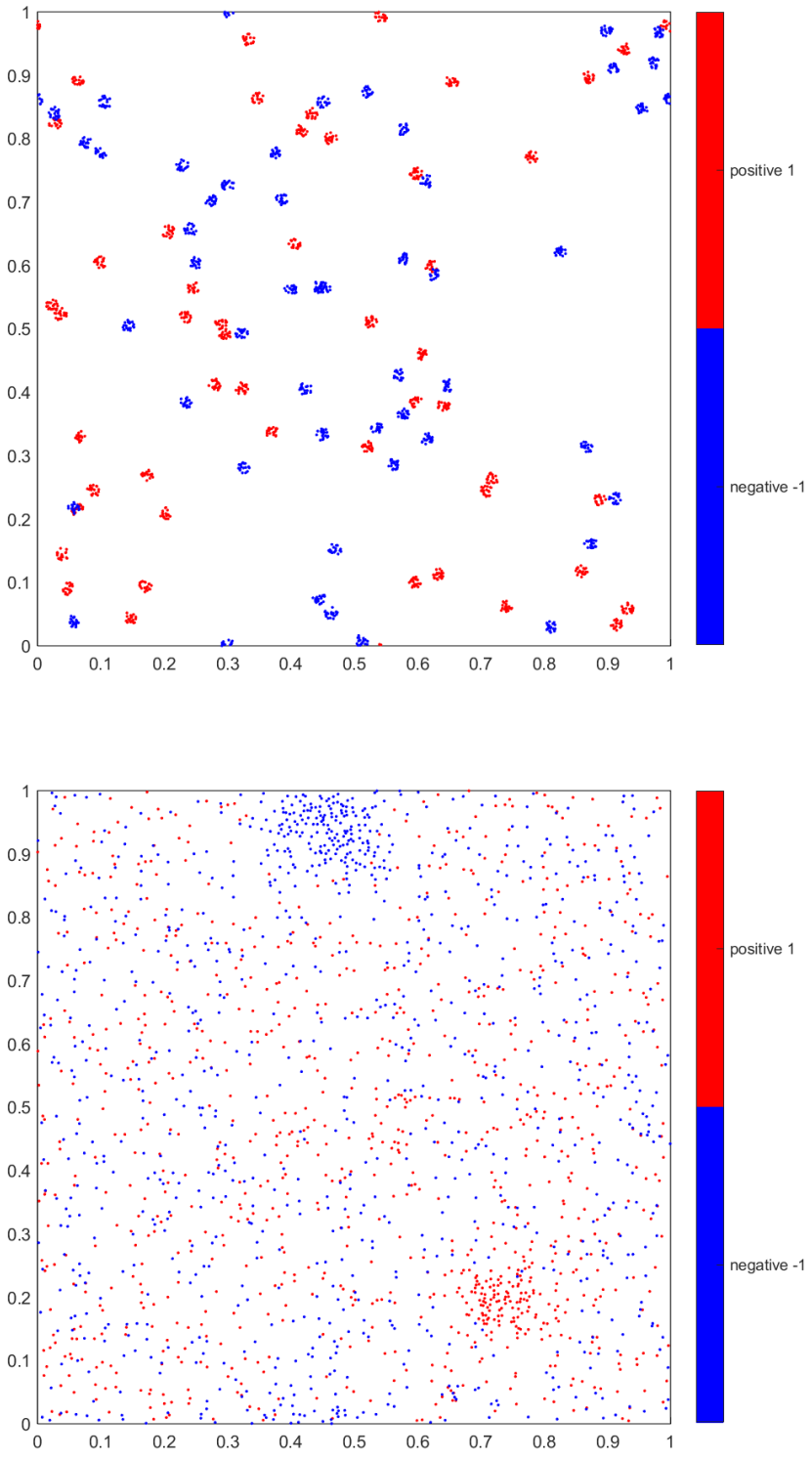

Figure 4.3: 100 small vortex patches (50 positive and 50 negative), with each patch contains 20 point vortices; after developing for 200 dimensionless time

$\mathcal{H}_{U,V}$ can be expressed as:

$$\mathcal{H}_{U,V} = \sum_{i\in U}\sum_{j\in V}\sum_{\boldsymbol{n}} \frac{\Gamma_i\Gamma_j}{4\pi^2|\boldsymbol{n}|^2}\exp\big(2\pi i\boldsymbol{n}\cdot(\boldsymbol{x}_i-\boldsymbol{x}_j)\big), \quad \boldsymbol{n}\in\mathbb{Z}^2, \boldsymbol{n}\neq(0,0) \tag{4.5}$$

Since V is randomly distributed vortices with the same number of positive vortices and negative vortices, for every point vortex $i \in U$, the interaction energy of i and all the $j \in V$ canceled each other and make the total interaction energy nearly zero:

$$\sum_{j\in V}\sum_{\boldsymbol{n}} \frac{\Gamma_i\Gamma_j}{4\pi^2|\boldsymbol{n}|^2}\exp\big(2\pi i\boldsymbol{n}\cdot(\boldsymbol{x}_i-\boldsymbol{x}_j)\big) \approx 0, \quad \boldsymbol{n}\in\mathbb{Z}^2, \boldsymbol{n}\neq(0,0) \tag{4.6}$$

Hence the total interaction energy between vortices in U and vortices in V is nearly zero:

$$\mathcal{H}_{U,V} \approx 0 \tag{4.7}$$

So we have:

$$\mathcal{H} \approx \mathcal{H}_U + \mathcal{H}_V \tag{4.8}$$

which means the system could be devided into two subsystems whose energy is additive. System U is the distribution of two opposite sign vortex patches, which is similar to case 2 and has negative temperature. System V is the distribution of randomly distributed different sign vortices, which is similar to case 1 and has infinity temperature.

If there are two different temperatures existing in the domain, it seems to be a problem why they did not balance each other. A possible explanation is: the infinity temperature is inactive. In Figure 2.5 we notice that near the center line, the temperature is diverging to both $+\infty$ and $-\infty$. When $T \to \infty$, $\frac{dS}{dE} = \frac{1}{T} \to 0$, which means the entropy will change little whether it loses or gains energy.

Another way to undertand this infinity temperature is to view it as **vacuum**. Recall in chapter 2, we have argued that the point vortices system is used to approximate the real continuous (or smooth) vorticity field. That is, we use $\sum_i^N \Gamma_i\delta(\boldsymbol{x}-\boldsymbol{x}_i)$ to approximate $\omega(\boldsymbol{x})$. We let N be big enough and Γ_i be small enough to achieve such a consequence: if the smallest scale in which we observe the vorticity field is l, then for every small area $|\Delta V| \sim l^2$ in the domain, we assume there are **quite a number of**

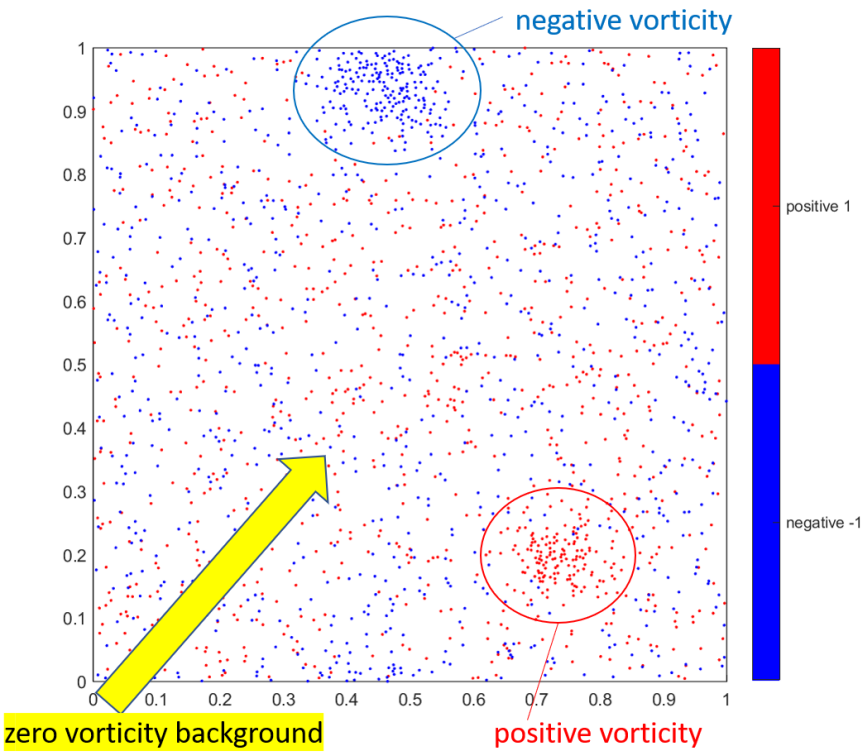

Figure 4.4: The final distribution of 2D turbulence case

point vortices in ΔV, such that the total vorticity of this small area is the summation of strength of point vortices inside of it:

$$\int_{\Delta V} \omega(x, y)\, dxdy \approx \sum_{\boldsymbol{x}_i \in \Delta V} \Gamma_i \tag{4.9}$$

With the above discussion, for the infinity temperature case which has randomly distributed different sign point vortices everywhere, we may say it represents a continuous vorticity field which is ZERO everywhere. This is because, if we randomly pick up an area ΔV which contains quite a number of point vortices, the total vorticity will be close to zero (see Figure 4.4). This may help us understand why there are no large structures formed in case 1: initially there is no vorticity in the domain.

Now we know in this case:

- the two vortex patches have negative temperature;
- the rest of the domain has infinity temperature, which is pretty similar to vacuum;
- negative temperature region has little interaction with the infinity temperature region.

4.3 Negative temperature in $\mathbb{R}^2$

4.3.1 Case 4: merging of two co-rotating vortex patches

In this subsection we will study the detailed mechanism of the merging of same sign vortex patches, and try to explain it with statistical mechanics analogy. First, from paper [13], we know that for any two vortices, whether their distribution is Gaussian or some other radial function, whether their sizes or strengths are equal or unequal, there is a specific distance, such that if they are closer than this distance, they tend to merge.

In Figure 4.5, we set up two vortex patches in the shape of circle, with radius $r = 0.1$, and their distance is $d = 0.3 = 3r$. Inside each circle, there are 1000 positive unit point vortices. For simplicity, here we use $\mathbb{R}^2$ domain instead of periodic boundary condition (in torus we need to make the total vorticity zero). We can see that the two vortex patches merged most of their parts after rotating less 180°. Before long, they totally merged together, leaving a bigger vortex patch, surrounded by many point vortices in a low density.

If we set the distance $d = 0.4 = 4r$, the two vortex patches will rotate with each other for a long time (about 160 dimensionless time), rotate for more than 20 circles, then merge together. They might never merge if the distance d is larger than $4r$. However, once the merging starts, it will finish very quick, usually no later than they rotate one circle with each other.

Now we may understand case 3 (2D turbulence) better. For many small vortex patches in the domain, because of the rather chaotic velocity field, it is possible for any two of them to be very close to each other. Once the distance is close enough, they will merge quickly.

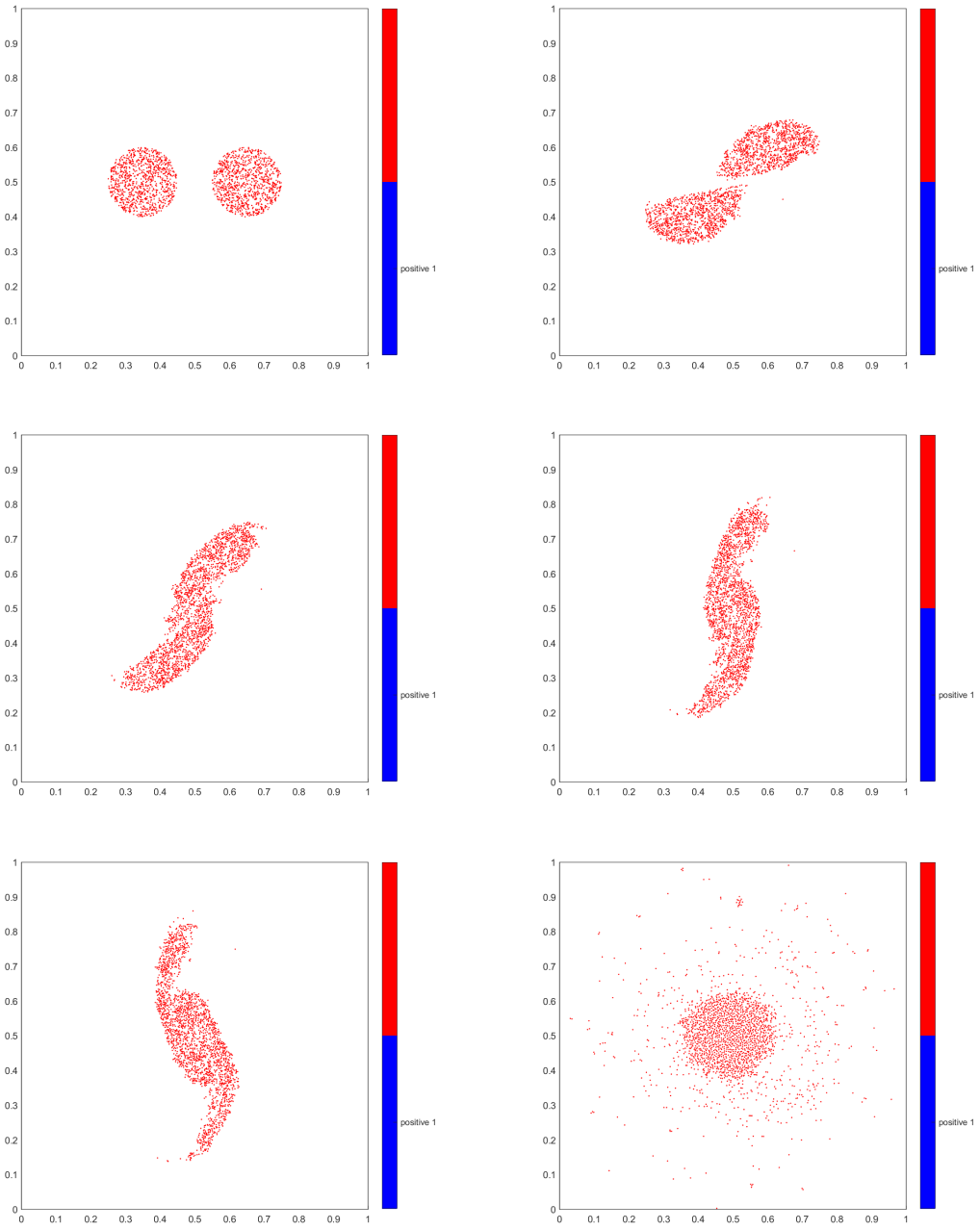

Figure 4.5: 2 big vortex patch circles, each with 1000 point vortices inside, at time 0, 0.4, 0.6, 0.8, 1, 20

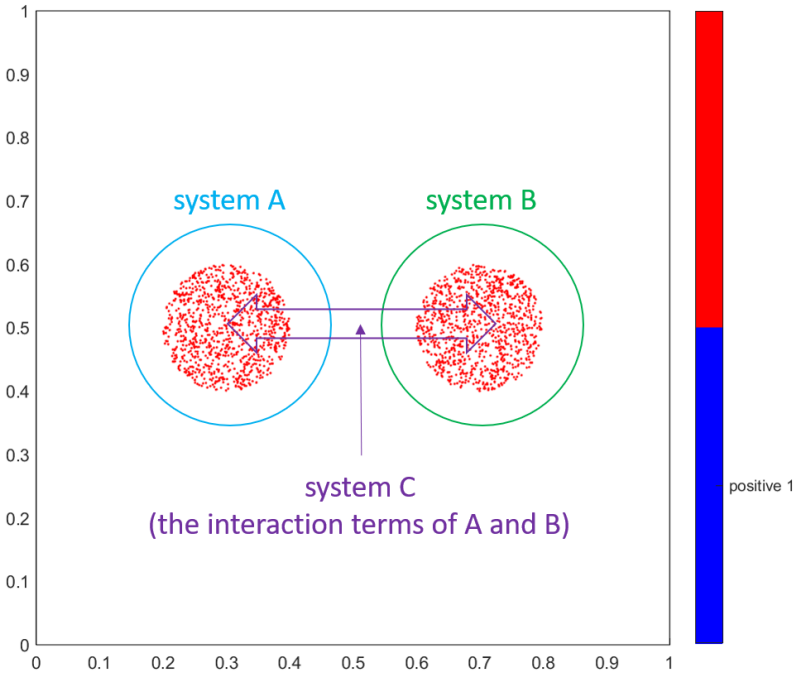

Figure 4.6: Schematic diagram of the 3 systems of two big vortex patches

4.3.2 The irreversibility of merging

As observed in simulation and many other experiments, this merging is irreversible. Once two vortices merge, they will never seperate in the future. Here we propose a heuristic explanation of the irreversibility based on statistical mechanics. Briefly speaking, the merging of two vortex patches (say A and B) is the balancing of the temperature of three objects: the vortex patch A, the vortex patch B, and the "interaction energy" system C. See Figure 4.6.

Assume there are N_A positive unit point vortices in the patch A, N_B positive unit point vortices in the patch A; the position of point vortices in A is $\boldsymbol{x}_i^A$, $1 \leq i \leq N_A$; the position of point vortices in B is $\boldsymbol{x}_i^B$, $1 \leq i \leq N_B$; then the energy (Hamiltonian) of the

total system is:

$$\begin{aligned}\mathcal{H} = &\sum_{1\le i<j\le N_A}\Big(-\frac{1}{2\pi}\log(|\boldsymbol{x}_i^A-\boldsymbol{x}_j^A|)\Big)+\sum_{1\le i<j\le N_B}\Big(-\frac{1}{2\pi}\log(|\boldsymbol{x}_i^B-\boldsymbol{x}_j^B|)\Big)\\ &+\sum_{i=1}^{N_A}\sum_{j=1}^{N_B}\Big(-\frac{1}{2\pi}\log(|\boldsymbol{x}_i^A-\boldsymbol{x}_j^B|)\Big)\\ =&E_A+E_B+E_C\end{aligned}$$

As two vortices are getting closer to each other, the term E_C will be bigger, while E_A and E_B will be smaller to conserve the total energy. By the analysis in last section, we know the clustering of vortices implies negative temperature, so the decrease of energy in patch A and B means the increase of entropy of patch A and B. This term C could be considered as the energy of two big point vortices A and B with vorticity N_A and N_B, so it also has negative temperature. The increase of energy in system C means the decrease of entropy of system C.

If the temperature satisfies:

$$0 > T_A > T_C$$

$$0 > T_B > T_C$$

then this energy transfering from A,B to C will let the entropy of total system increase. Finally when two vortex patches merged together, we might have:

$$T_A = T_B = T_C$$

So the temperature has been balanced. This might explain the irreversibility of merging.

4.3.3 Case 5: merging of many vortex patches

Now we increase the number of vortex patches in the $\mathbb{R}^2$ domain. In Figure 4.7, we set 1000 positive point vortices in the domain, with every 20 of them forming a little patch with radius 0.01 (so we have 50 patches), and let these patch randomly distribute inside a circle with radius 0.4. After developing for 100 dimensionless time, we will see most patches merged together, leaving only several big patches. This looks very similar to

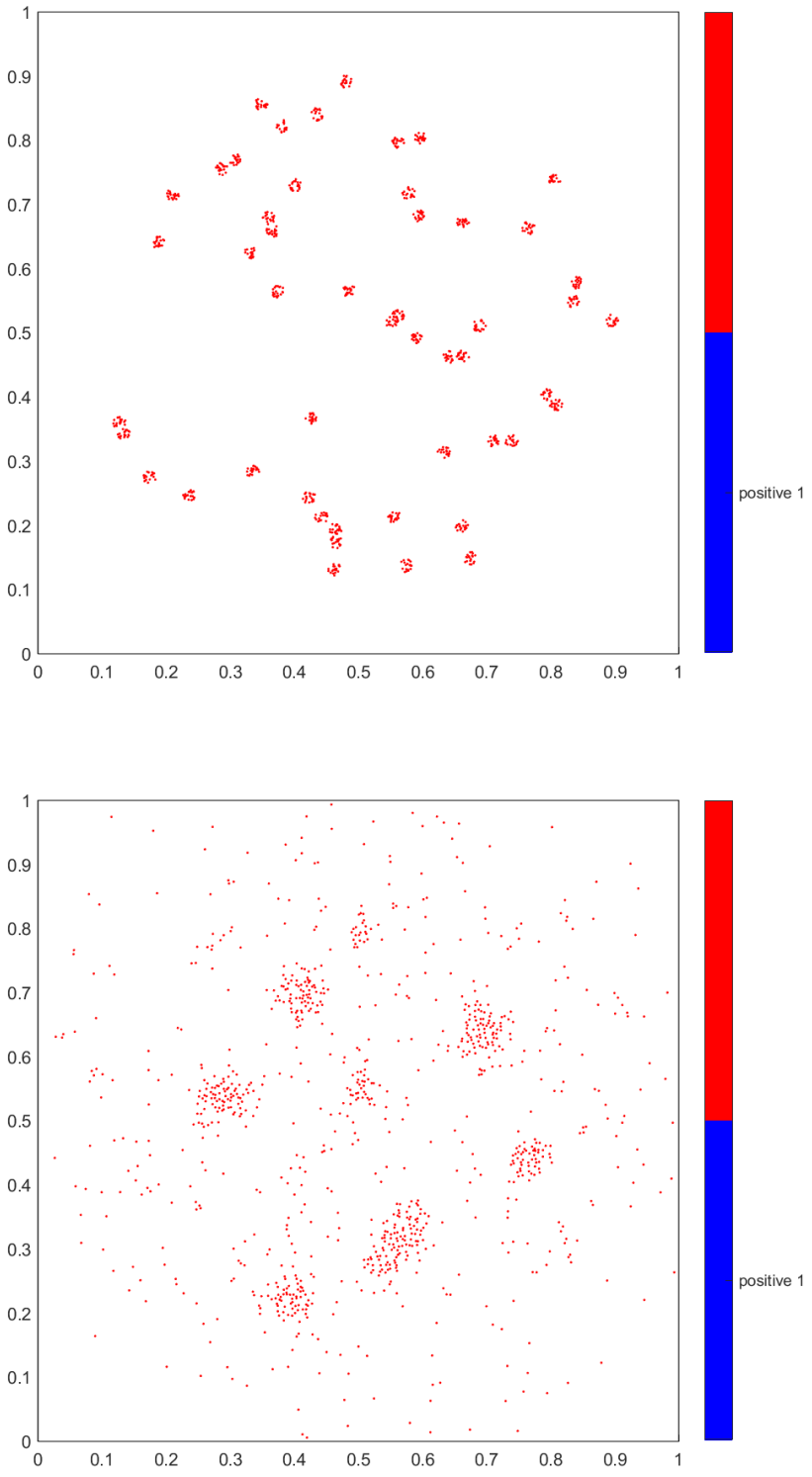

Figure 4.7: 1000 vortices, forming 50 small vortex patches; after developing for 100 dimensionless time

the formation of galaxy. By the analysis of the previous subsection, we may regard such formation of large vortex as the balancing of temperature (which is negative, of course).

4.4 Positive temperature

In Figure 2.5 we observe that as energy $E < E_m$, our system may have positive temperature. Since we have already see the situation of negative temperature (clustering of same sign vortices) and infinity temperature (randomly distributed different sign vortices), we may wonder what positive temperature case looks like. By looking at equation (4.1) and (4.2), we can let two opposite sign vortices be very close to each other to let the energy be sufficiently small. Specifically, we know the randomly distributed different sign vortices in torus is in infinity temperature, and the average distance between each one and its nearest one is $d \approx \sqrt{V/N}$, where V is the area of the domain, N is the number of point vortices. Then, we can let every pair of vortices with different sign be very close to each other, with the average distance $d' \ll d$. In this situation, the energy (in the Hamiltonian sence) will be much smaller than the randomly distributed vortices situation.

4.4.1 Case 6: many dipoles

Here we dig into the property of such positive temperature case. As shown in Figure 4.8, we set 2000 unit point vortices in the torus domain, with half of them positive and half of them negative. We let them form 1000 dipoles (the pair of one positive point vortex and one negative point vortex that are close to each other), and the distance between the vortex pair of each dipole is 0.001.

If we let the system run, we will see these dipoles moving in a straight line, similar to particles with a momentum. They will collide with each other, which makes some of them faster, while some of them slower. The distance between the vortex pair of faster dipole is closer, which means the size of the dipole is smaller. The distance between the vortex pair of slower dipole is farther away from each other, and may dissipate to the background (totally seperated). After running for a relatively long time (100 dimensionless time), we will see that many dipoles are seperated, but there are still many dipoles left in the domain. In Table 4.1, we compared the number of dipoles of

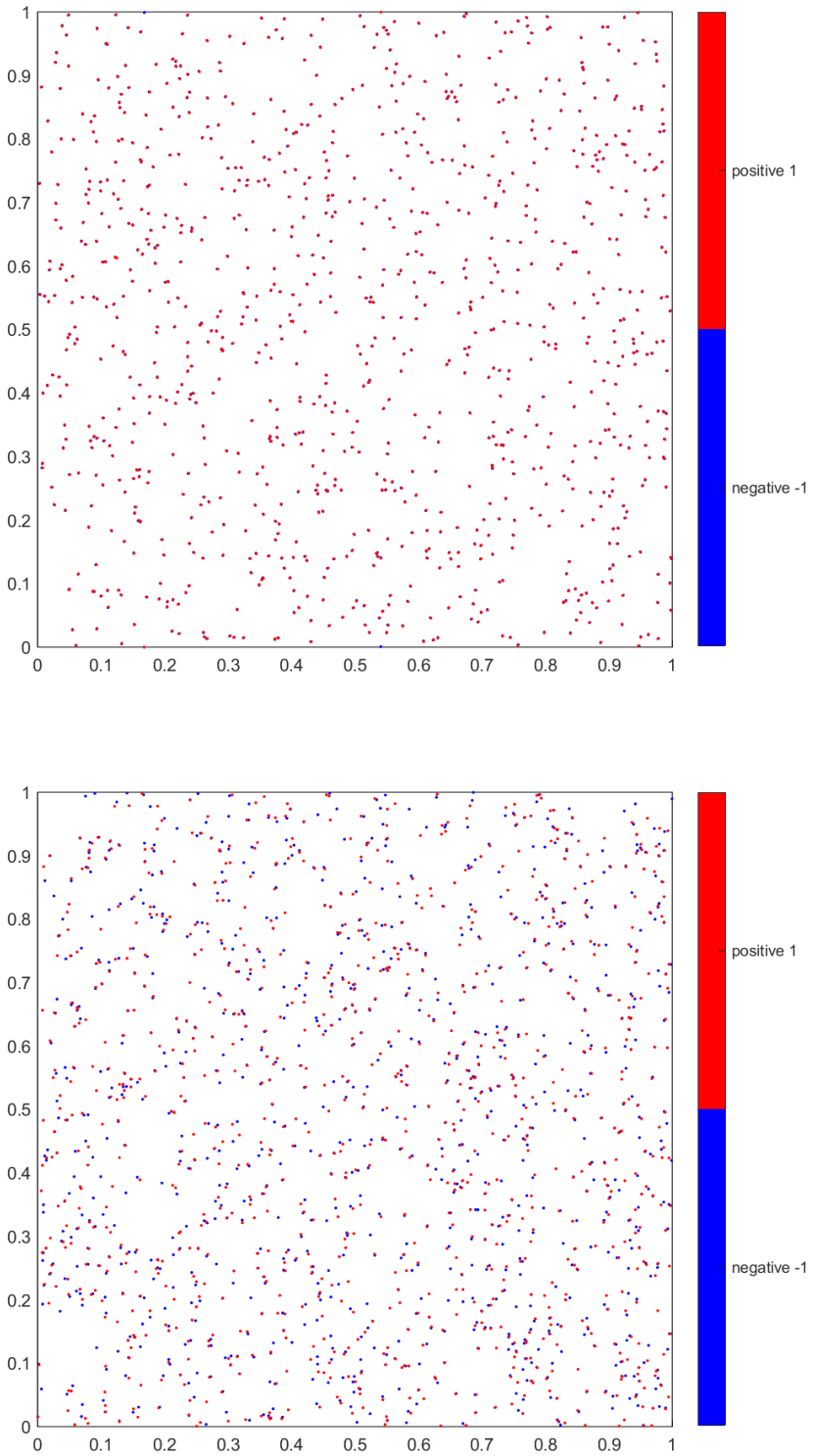

Figure 4.8: 1000 vortex dipoles in torus; after developing for 100 dimensionless time

case 6 and case 1 (randomly distributed vortices), and find that the former is much greater than the latter.

distance less than	0.001	0.002	0.003	0.004	0.005
number of dipoles in case 6	139	288	404	502	610
number of dipoles in case 1	12	29	51	79	127

Table 4.1: The number of dipoles in which the distance of vortex pair is small (time 100 in case 6 v.s. time 100 in case 1)

In this case, there is still no large structures formed in the domain, like the infinity temperature case.

4.4.2 Case 7: free expansion

The "high speed particles (dipoles)" represents the property of positive temperature situation, while the "large vortex patch" represents the property of negative temperature situation. A main difference between these two properties is that the "large vortex patch" is condensed, while the "high speed particles (dipoles)" could expand freely.

We may use the following case to elaborate it. In Figure 4.9, we set 1000 unit vortices (half positive half negative) randonly distribute inside a small square with side length 0.1, in the center of a torus. At the beginning, many high speed particles (dipoles) move very fast from the small patch, and the square patch begins to distort and expand. As time goes by, the patch becomes bigger and less dense, with many dipoles surrounding it in the whole domain. After 100 dimensionless time, the patches disappeared or dissipated to the whole domain, while there are still many fast moving dipoles.

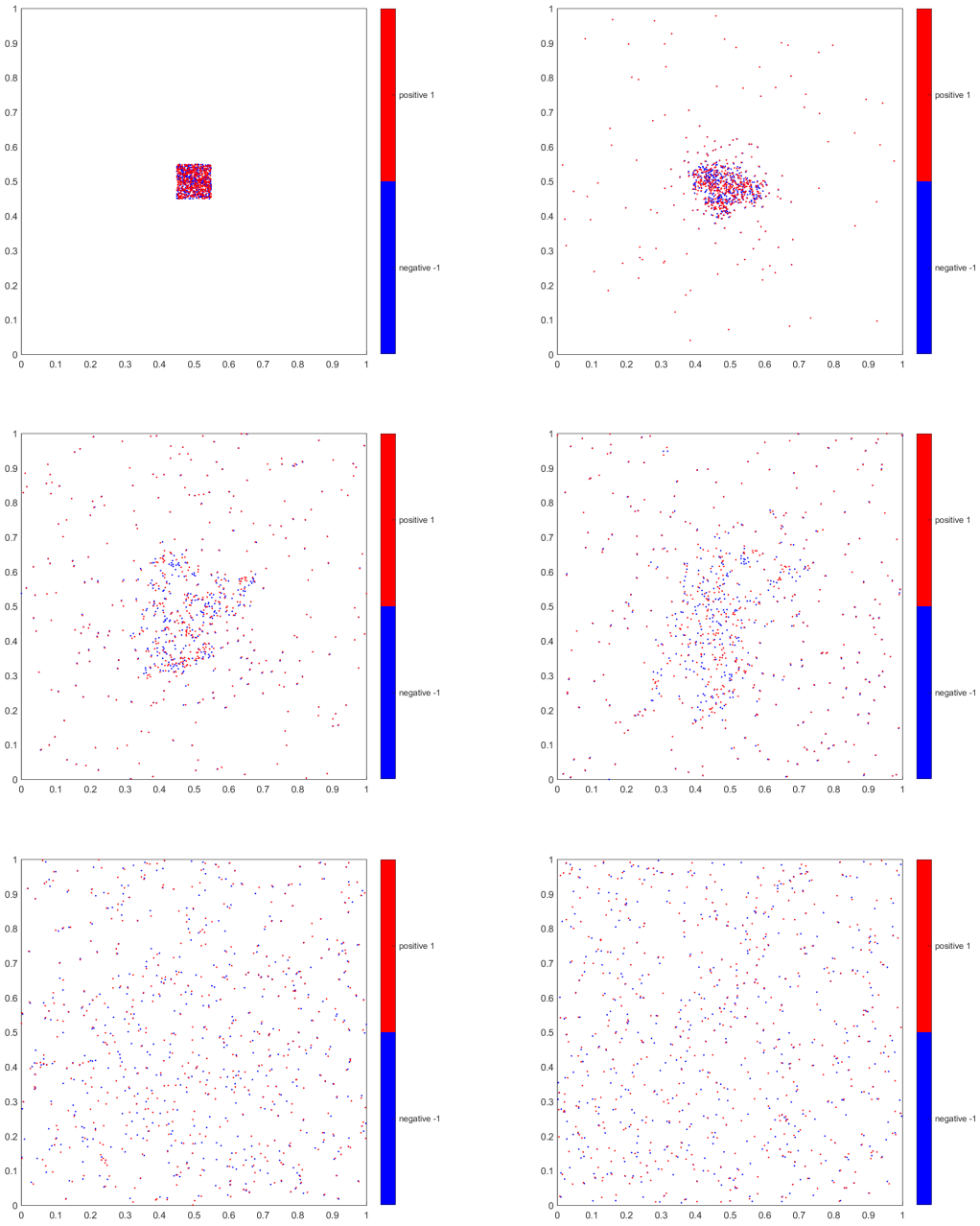

Figure 4.9: Free expansion of randomly distributed vortices in a small square, at time 0, 1, 5, 10, 50, 100

We can quantify the energy of this case by the same idea of randonly distributed vortices in the whole domain, and get the energy expression similar to the equation (4.3). Denote our small square's area $V' \ll V$, then our energy is :

$$\mathcal{H} \approx \frac{N}{4\pi}\log(\sqrt{V'}) \ll \frac{N}{4\pi}\log(\sqrt{V}) \approx \mathcal{H}_{random} \approx E_m \tag{4.10}$$

Since the energy of this case is much small than E_m, by Figure 2.5 we know it has positive temperature.

4.4.3 Case 8: neutralization of positive temperature and negative temperature

We have already know that infinity temperature is like vacuum, so it has nothing to do with the "large vortex patch" or "high speed particles (dipoles)". We may wonder, what will happen if we put the "large vortex patch" and "high speed particles (dipoles)" together.

distance less than	0.001	0.002	0.003	0.004	0.005
number of dipoles in case 6	139	288	404	502	610
number of dipoles in case 1	12	29	51	79	127
number of dipoles in case 8	9	20	40	69	130

Table 4.2: The number of dipoles in which the distance of vortex pair is small, at time 100 in case 6, case 1, case 8

In Figure 4.10, we set 2000 point vortices in the torus, with half in 0.001 and half in -0.001. In the left domain we set 875 pairs of different sign vortices, with each pair

has distance 0.001. In the right domain we set two big vortex patch, with each patch contains 125 same sign vortices. After running for 100 dimensionless time, we see the number of dipoles is in the same magnitude of case 1 (randomly distributed vortices), in Table 4.2. Hence we conclude that all the dipoles are destroyed by "large vortex patch". This is consistent with our view of balancing of different temperatures.

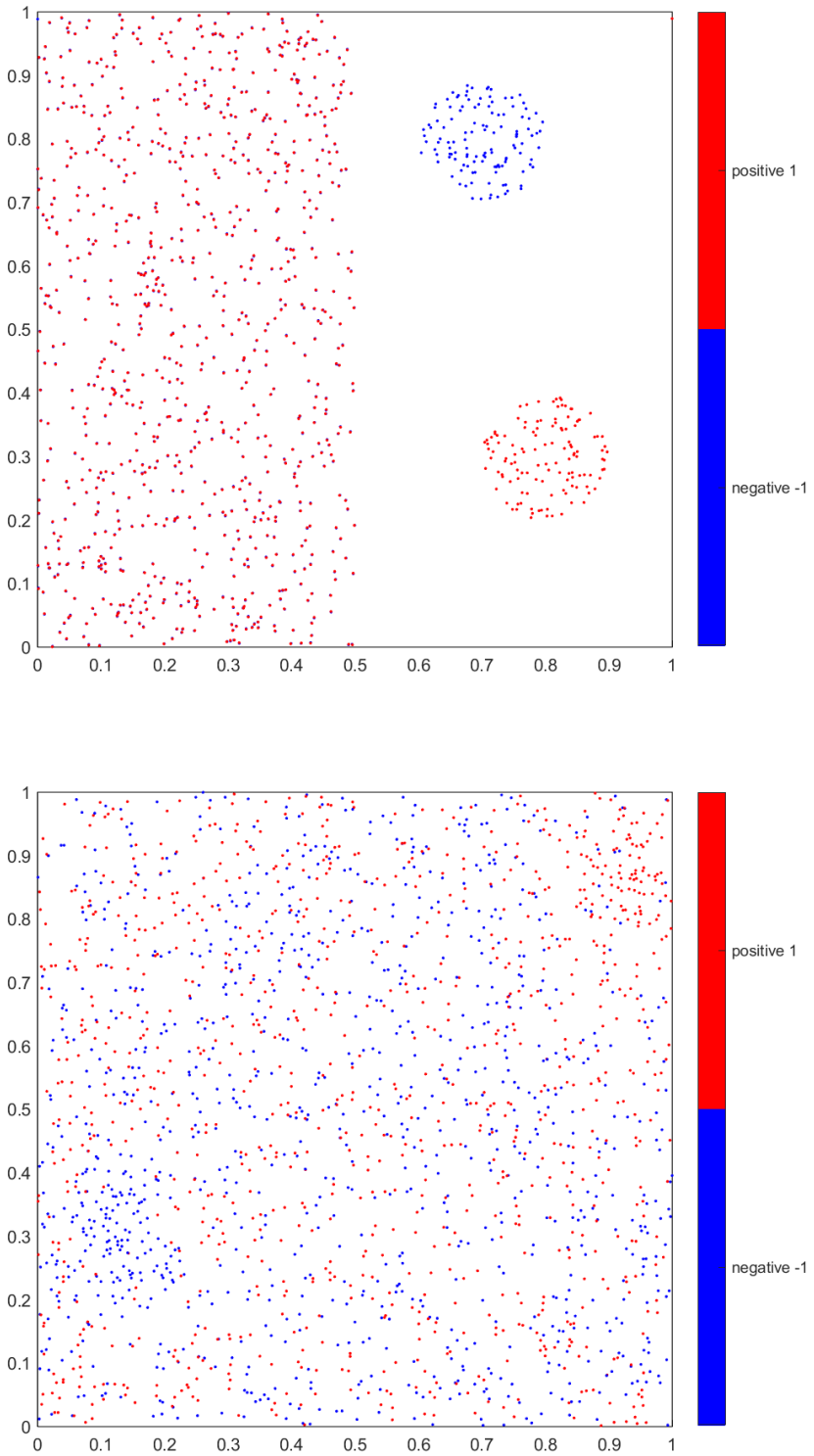

Figure 4.10: 2000 vortices, with 1750 in the left domain forming dipole, and 250 in the right domain forming vortex patches; after developing for 100 dimensionless time

Chapter 5

A new point of view: energy shell thickness

In chapter 2 we briefly mentioned the "energy shell" , which is a hypersurface in phase space $(\mathbb{P}, \mathbb{Q})$ which satisties $\mathcal{H}(\mathbb{P}, \mathbb{Q}) = E$. Energy shell could have **irregular "thickness"** (Figure 5.1) [14]. This is a littile hard to understand because as $\delta E \to 0$, every part of the energy shell tends to be arbitrarily thin. But we can imagine that some part of the energy shell's thickness decreases slower than other parts, so that even though they both aproach 0, the former could be bigger than the latter.

In microcanonical ensemble, $\rho = Const.$ inside the energy shell. This tells us, the thicker part of the energy shell shall have more probability to be seen (or to appear) than the thinner part. In other word, the system would be more likely to stay in a microstate of thicker region of the energy shell. Indeed, we are assuming there is a

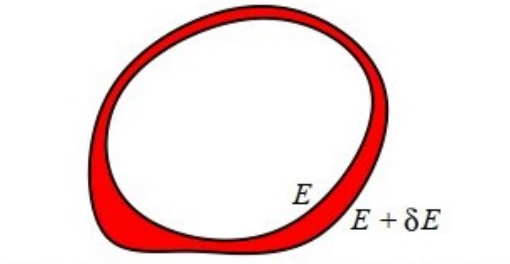

Figure 5.1: Energy shell.

possibility density of the surface of fixed energy in phase space, and we want to find the place with the highest density. More precisely, we want to find a $(\mathbb{P}, \mathbb{Q})$ that maximizes $|1/\nabla\mathcal{H}(\mathbb{P}, \mathbb{Q})|$.

Based on this idea, we may explain the merge of vortices.

5.1 The simplest example

Assume we just have two vortices, in a 1D domain $[0, 1]$, and the Hamiltonian is defined by:

$$\mathcal{H}(x_1, x_2) = -\ln|x_1 - x_2| \tag{5.1}$$

where $x_1, x_2 \in [0, 1]$.

This example looks puzzling at first glance. How can point vortices be confined in 1D? How can the vortices move? The explanation is that in statistical mechanics we do not care how the particles move. Instead, we focus on the probability of a particle to exist in a specific position of the domain. Theoretically we need to analyze point vortices in 2D torus, but then with 2 vortices our phase space is 4D (also the Hamiltonian is complicated), which makes it hard to draw the picture of the phase space. By analyzing this example, we could gain some heuristics about the structure of the phase space, and the shape of energy shell.

In the framework of microcarnonical ensemble, we were able to use the Hamiltonian to get our phase space volume $\Omega(E)$, and even to calculate the temperature.

The phase space of this example is a 2D square, see Figure 5.2. The energy defined by Hamiltonian is 0 in the upper-left and lower-right corner, and is infinity in the line of $x_1 = x_2$. By equation (2.36) we have:

$$\int_0^E \Omega(E')\, dE' = \int_{0<\mathcal{H}(x_1,x_2)<E} dx_1 dx_2 \tag{5.2}$$

Look at the Figure 5.2, the right-hand-side of the above equation is equal to the addition of a upper-left triangle and a lower-right triangle with cathetus c satisfies $E = -\ln(1-c)$.

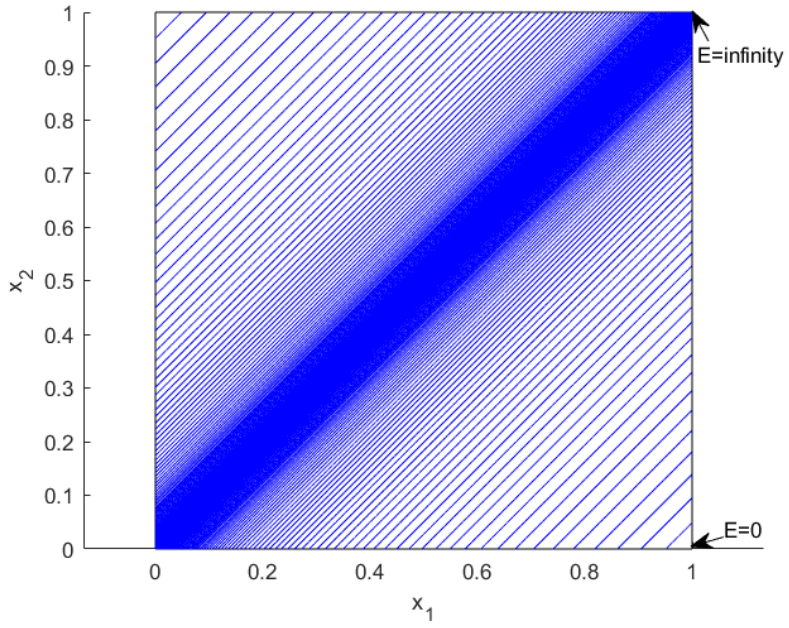

Figure 5.2: Phase space of two vortices system in 1D; the blue line quantifies the thickness of energy shell.

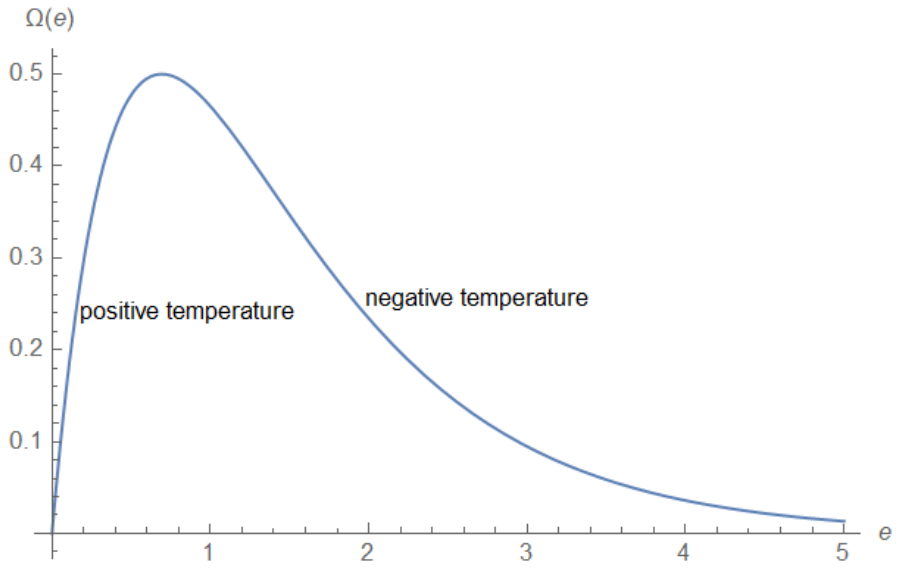

Figure 5.3: Phase space volume $\Omega(E)$ of two vortices system in 1D

Hence $c = 1 - \exp(-E)$, and

$$\int_0^E \Omega(E')\, dE' = \big(1 - \exp(-E)\big)^2$$

$$\Rightarrow \quad \Omega(E) = 2\big(1 - \exp(-E)\big)\exp(-E) \tag{5.3}$$

In Figure 5.3 we can plot the function of $\Omega(E)$. We find that $\Omega(E)$ first increases, reaches its maximum at $E = \ln 2$, then decreases and approaches to 0. To understand this, we can look at the energy shell in Figure 5.2. We notice that as $|x_1 - x_2| \to 0$, which means as the energy $E \to \infty$, the energy shell will become thinner and thinner. This is the reason why the phase space volume $\Omega(E)$ decreases as energy $E \to \infty$. As for the beginning increasing of $\Omega(E)$, if we look at the lower-right corner of Figure 2.3, we will find, even though the energy shell becomes thinner as E grows, the length of the shell becomes longer. Hence, although the thickness of the shell is decreasing, the area of the shell is increasing, making the whole volume of the shell increase.

Remember the definition of phase space volume $\Omega(E)$:

$$\Omega(E) = \lim_{\delta E \to 0^+} \frac{1}{\delta E} \int_{E < \mathcal{H}(\mathbb{P},\mathbb{Q}) < E + \delta E} d\mathbb{P} d\mathbb{Q} \tag{5.4}$$

It seems the phase space volume is the area of an (N-1) dimension surface of our N dimention phase space. But it is not. The phase space volume contains both the information of area and thickness.

From this example, we find that when two vortices are very close to each other, the energy shell will be very thin. We can also understand this by imagining these two vortices can vibrate along the center of them. This vibration is within a tiny energy deviation δE. As the distance becomes smaller (the energy E becomes bigger), the amplitude for them to vibrate will be smaller, making the "free space" for them to roam be smaller.

5.2 Energy shell thickness

In Figure (5.2), we can see for every specific energy shell, the thickness is even. That is not true when we have more than two vortices. For example, if we have three positive vortices (or just call them particles) in $[0, 1]$, let the Hamiltonian be:

$$\mathcal{H}(x_1, x_2, x_3) = -\ln|x_1 - x_2| - \ln|x_1 - x_3| - \ln|x_2 - x_3| \tag{5.5}$$

where $x_1, x_2, x_3 \in [0, 1]$.

The total phase space will be a $[0, 1] \times [0, 1] \times [0, 1]$ cube. We may also have that $\Omega(E) \to 0$ as $E \to \infty$, which brings us negative $\Omega'(E)$ or negative temperature at high energy. But the shape of the energy shell is quite hard to describe.

By the logic of microcarnonical ensemble, the probability is even inside the energy shell (equation 2.35). So we want to know where is the thickest position of the shell. That may be the place the system likes to stay, and represents the evolution direction.

A **method to quatify the thickness** d of a specific position (x_1^*, x_2^*, x_3^*) is by calculating:

$$d = \min_i \left(\left| 1 / \left(\frac{\partial \mathcal{H}}{\partial x_i} \Big|_{(x_1^*, x_2^*, x_3^*)} \right) \right| \right) \tag{5.6}$$

Figure 5.4 may help us understand the idea of equation (5.6). In this figure we assume the energy shell is in the shape of circle, and our coordinate is Cartesian. Then in a random point of our fixed energy circle (the blue dot), we can find the distance from this point to the the $E + \delta E$ energy circle in both x direction and y direction, which

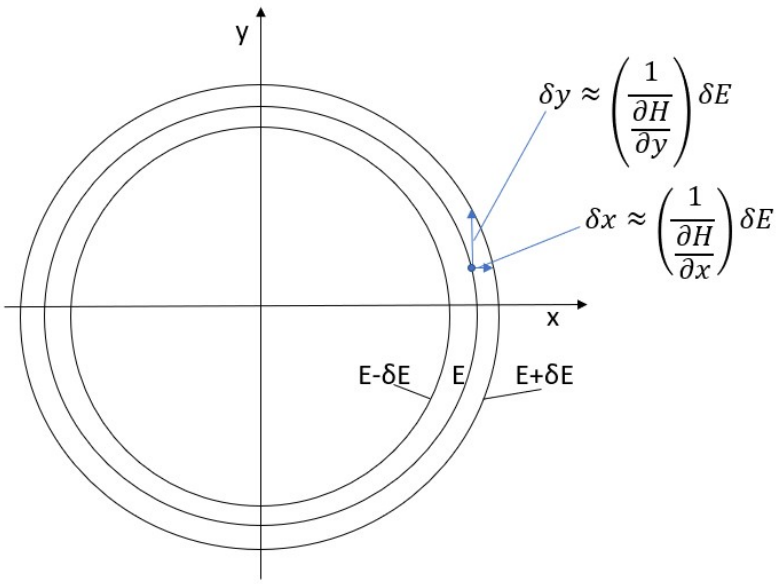

Figure 5.4: Schematic diagram of the method to quantify the thickness of energy shell

are δx and δy. However, both δx and δy are bigger than the real thickness between E and $E + \delta E$. If we can use cylindrical coordinates (r, θ) to express $\mathcal{H}$, then a more appropriate quantification of this thickness is $\delta r = 1/\left(\frac{\partial \mathcal{H}}{\partial r}\right) \cdot \delta E$. But if we could only use (x, y) to express $\mathcal{H}$, then $\min(\delta x, \delta y)$ is almost the best choice to quantify the thickness.

This method could be generalized to multiple vortices in 2D domain. For $\mathcal{H}(x_1, x_2, \cdots, x_n)$, the thickness d of a specific position $(x_1^*, x_2^*, \cdots, x_n^*)$ is by calculating:

$$d = \min_i \left(\left| 1/\left(\frac{\partial \mathcal{H}}{\partial x_i} \Big|_{(x_1^*, x_2^*, \cdots, x_n^*)} \right) \right| \right) \tag{5.7}$$

5.3 Three vortices in 1D

Now let us analyze the three vortices system in 1D, and try to find at what microstate the thickness will reach its maximum. Assume we have three same sign vortices in $\mathbb{R}$. The Hamiltonian is:

$$\mathcal{H}(x_1, x_2, x_3) = -\ln|x_1 - x_2| - \ln|x_1 - x_3| - \ln|x_2 - x_3| \tag{5.8}$$

where $x_1, x_2, x_3 \in \mathbb{R}$. Here we didn't limit our domain in $[0, 1]$, because later we will see that the thickness doesn't require the boundedness of phase space. (If we want to calculate entropy or temperature, we need the boundedness.)

Without loss of generality, let's assure $x_1 > x_2 > x_3$, and $\mathcal{H} = -\ln 2$. Denote $h_1 = x_1 - x_2$, $h_2 = x_1 - x_3$, $h_3 = x_2 - x_3$, then we have:

$$h_1 + h_3 = h_2 \tag{5.9}$$

$$h_1 h_2 h_3 = 2 \tag{5.10}$$

From equation (**??**), we have:

$$d_1 \equiv \left| 1/\Big(\frac{\partial \mathcal{H}}{\partial x_1}\Big) \right| = \left| 1/\Big(\frac{1}{h_1} + \frac{1}{h_2}\Big) \right| \tag{5.11}$$

$$d_2 \equiv \left| 1/\Big(\frac{\partial \mathcal{H}}{\partial x_2}\Big) \right| = \left| 1/\Big(\frac{1}{h_1} - \frac{1}{h_3}\Big) \right| \tag{5.12}$$

$$d_3 \equiv \left| 1/\Big(\frac{\partial \mathcal{H}}{\partial x_3}\Big) \right| = \left| 1/\Big(\frac{1}{h_2} + \frac{1}{h_3}\Big) \right| \tag{5.13}$$

It's easy to check $d_2 > \min\{d_1, d_3\}$. Also from (5.9) (5.10), we have: $h_3 = \frac{-h_1 + \sqrt{h_1^2 + 8/h_1}}{2}$, $h_2 = \frac{h_1 + \sqrt{h_1^2 + 8/h_1}}{2}$. Hence, to find at what point we have the thickest energy shell, we just need to find a h_1^* s.t. $d(h_1) = \min\{d_1(h_1), d_3(h_1)\}$ reaches its maximum at h_1^*.

By plotting $d_1(h_1)$ and $d_2(h_1)$ (Figure 5.5), we can find that $\min\{d_1(h_1), d_3(h_1)\}$ reaches its maximum at $h_1^* = 1$. Hence, when $h_1 = h_3 = 1$, $h_2 = 2$, we reaches our the thickest position of energy shell of $\mathcal{H} = -\ln 2$, which means our system reaches its most probable state (Figure 5.6).

This example tells us, for three same sign vortices in 1D, with fixed enegy $\mathcal{H} = E_0$, the most probable state is the symmetric state. If our system is developing to the direction of thicker position of energy shell, then at whatever initial state, it will finally reach the symmetric state and stay there.

For example, if the initial state is $h_1 = 0.1$, $h_2 = 4.5224$, $h_3 = 4.4224$, then it satisfies (5.9) (5.10), which means the energy of the system is $E = -\ln 2$. As time goes by, the system finally will be in the state that $h_1 = h_3 = 1$, $h_2 = 2$.

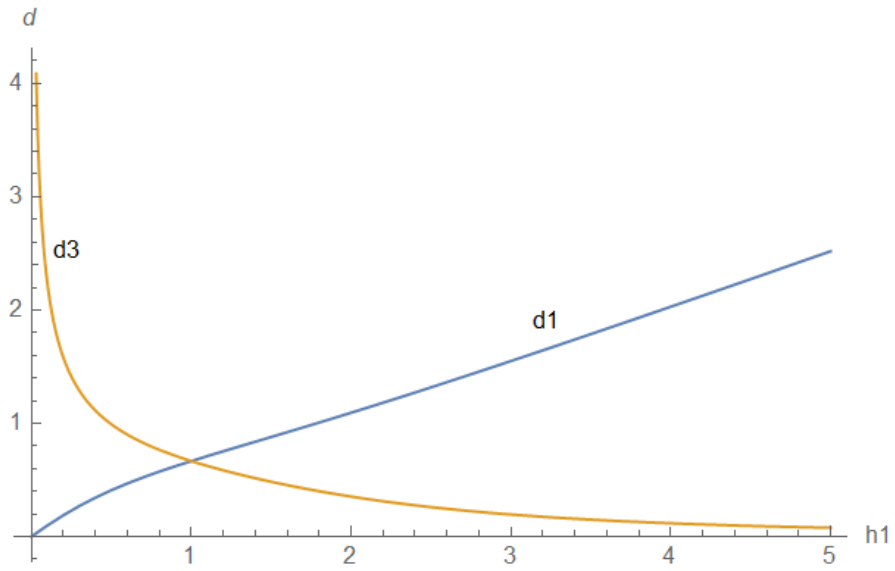

Figure 5.5: Function of $d_1(h_1)$ and $d_2(h_1)$

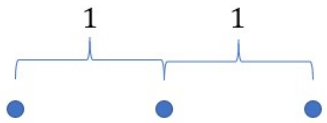

Figure 5.6: The most probable state of three vortices in 1D

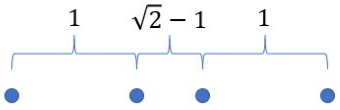

Figure 5.7: The most probable state of four vortices in 1D

5.4 Four vortices in 1D

If we have four same sign vortices in $\mathbb{R}$, let the Hamiltonian be:

$$\begin{aligned}\mathcal{H}(x_1,x_2,x_3,x_4) = &-\ln|x_1-x_2|-\ln|x_1-x_3|-\ln|x_1-x_4| \\ &-\ln|x_2-x_3|-\ln|x_2-x_4|-\ln|x_3-x_4|\end{aligned} \tag{5.14}$$

By similar analysis to the three vortices case, we can find the most probable state is: $x_1 - x_2 = 1$, $x_2 - x_3 = \sqrt{2}-1$, $x_3 - x_4 = 1$. See Figure 5.7. In addition, we found in this distribution

$$\left|1/\left(\frac{\partial\mathcal{H}}{\partial x_1}\right)\right| = \left|1/\left(\frac{\partial\mathcal{H}}{\partial x_2}\right)\right| = \left|1/\left(\frac{\partial\mathcal{H}}{\partial x_2}\right)\right| = \left|1/\left(\frac{\partial\mathcal{H}}{\partial x_4}\right)\right| \tag{5.15}$$

which means the energy shell thickness is equal in all directions.

5.5 Many vortices in 2D

The most probable state in 1D with four point vortices may give us the heuristic to explain the merging of vortex patches in 2D. See Figure 5.8, if initially we have 2 vortex patches far away from each other (the left distribution), then by the assumption that they tend to evolve to the most probable state, finally these two pairs would be in the right distribution, with density of vortices near the center higher than the density of vortices far away from the center.

Here is another case to elaborate this "higher density near the center". In Figure 5.9, we set 1000 point vortices in the $\mathbb{R}^2$, forming the shape of a ring. After developing

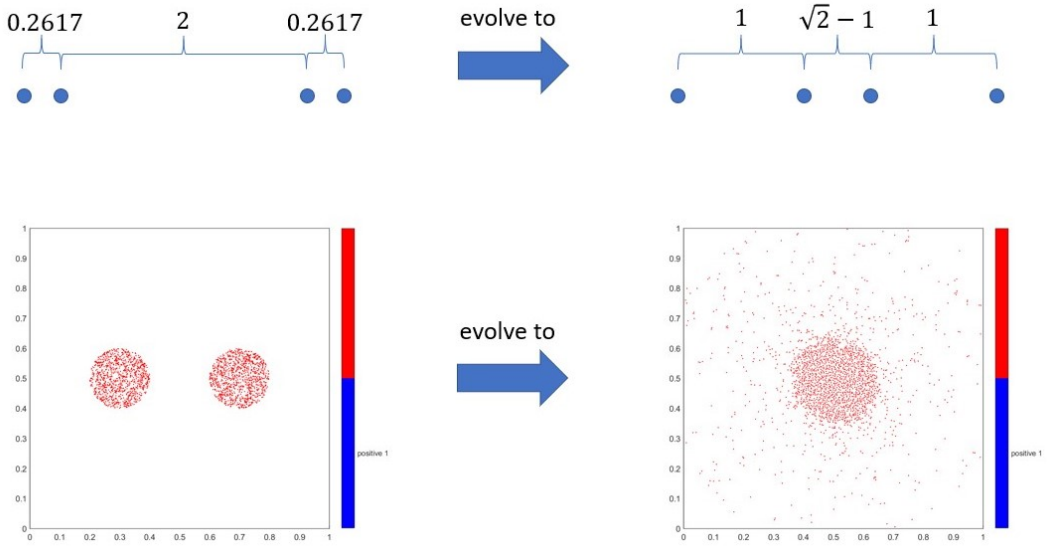

Figure 5.8: Evolution to most probable state

for 50 dimensionless time, the ring collapses into an axisymmetric distribution, with the density of vortices near the center higher than the density of vortices far away from the center. This decreasing of density from the center has been proved in [15]

If we expand equation (5.15) to 2D, it implies that the absolute value of velocity of every point vortices is equal. Indeed, by equation (5.7) the fastest vortex will decide the thickness of energy shell of this state. To let the thickness be small, we need to let the fastest vortex be as slow as enough. Since the energy conserved, some vortex becomes slower means other vortices become faster, and finally we may let every point vortex have the same speed.

This conclusion above is not always right in experiments and simulations, but it may provide a view to understand why vortex patches tend to merge, and why the final big vortex has higher density near the center.

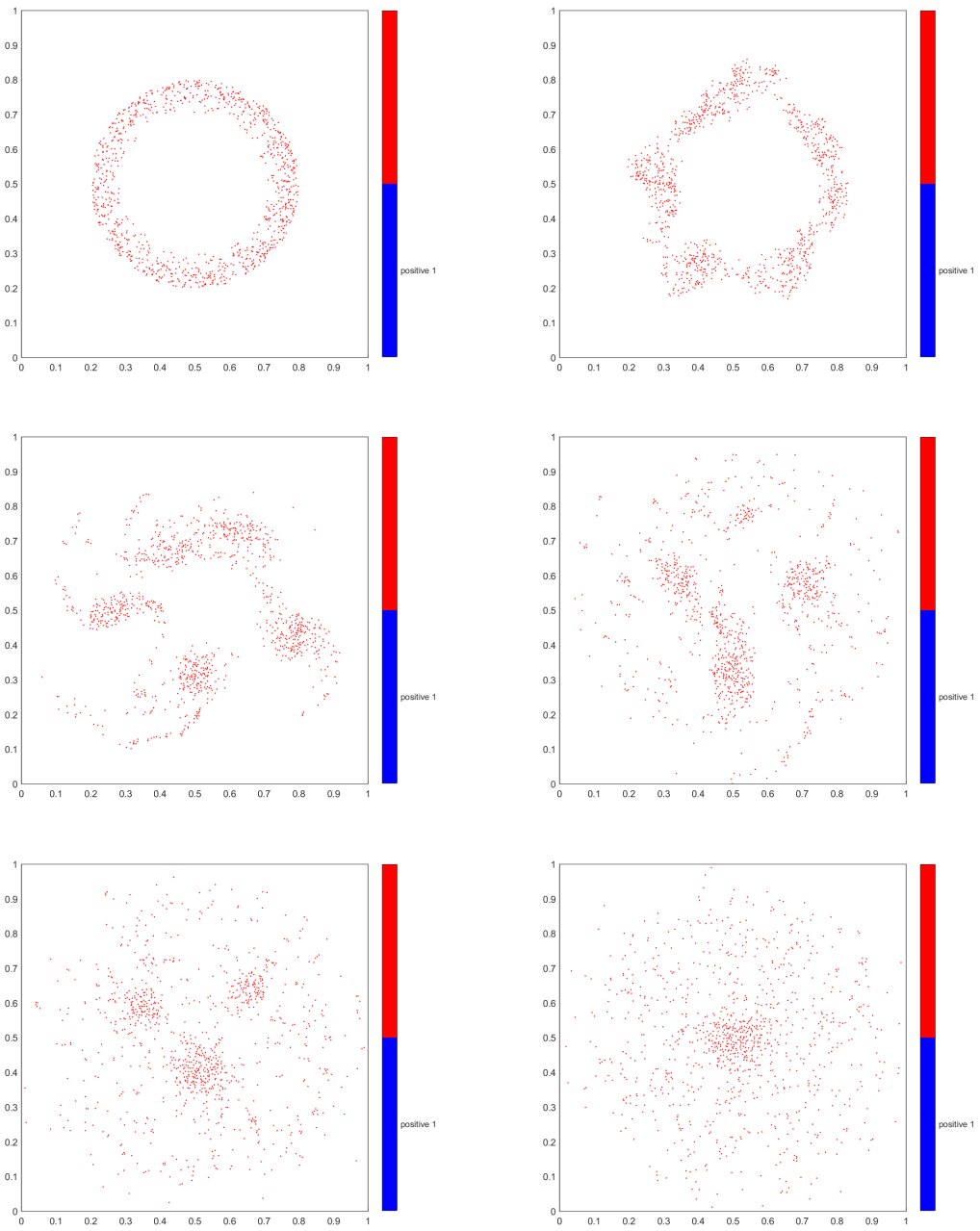

Figure 5.9: Vortex patch in the shape of ring in $\mathbb{R}^2$, at time 0, 2, 5, 10, 20, 50

Chapter 6

Conclusion

We studied the formation of large scale vortex structures in 2D turbulence using numerical simulations and the theory from statistical mechanics. We first demonstrated the suitability of using point vortex system to study the long-term evolution of 2D Euler equation. Then we analyzed the phase space volume function $\Omega(E)$ for point vortex system in torus. Following Onsager's "negative temperature" idea, we find the point vortex system in torus behaves in a very consistent way with negative temperature property when the energy of the system is sufficiently high. The graph of $\Omega(E)$ also implies the system would have infinity temperature near the central line $E = E_m$ of $\Omega(E)$, and would have positive temperature when the energy is sufficiently small.

To study the 2D turbulence phenomenon, we developed a numerical algorithm to calculate the velocity of point vortex system on torus, and controled the truncation error to be acceptable.

We analyzed different phenomenon in our simulation. For randomly distributed vortices, we find it would stay random. This can be explained by regarding the vorticity field as zero. We name it "infinity temperature" because its entropy would change little when gaining or losing energy. For initial distribution that already has small scales of coalescence of same sign vortices, we observe the merging of small vortex patches into big vortex patches. The merging process is also studied in $\mathbb{R}^2$. The irreversibility of the merging is explained by a heuristic "temperature balancing" idea. We constructed cases with positive temperature, which is characterized by fast moving dipoles. We find the positive temperature and negative temperature systems could neutralize each other.

Finally, we provide a new idea to understand the merging of vortex patches. We assume the point vortex system would evolute to the state which has the thickest energy shell thickness in the phase space. Then we analyzed the phase space volume $\Omega(E)$ of two, three and four vortices in one dimensional space, and gave an approximate formula to calculate the energy shell thickness in every point of phase space. The most probable state of four vortices in 1D implies that the merging of vortex patches in 2D is the evolution to most probable state. It also impiles the density of vortex patches in higher near the center, which is consistent with observation.

References

[1] C. E. Wayne, *Vortices and Two-Dimensional Fluid Motion*, Not. AMS **58** (2011), 1–19

[2] J. Miller, B. Weichman and M. C. Cross, *Statistical mechanics, Euler's equation, and Jupiter's Red Spot Jonathan*, Phys. Rev. A **45** (1992), 2328–2359

[3] S. B. Pope, *Turbulent Flows*, Cambridge: Cambridge University Press. (2000)

[4] R. H. Kraichnan, *Inertial ranges in two-dimensional turbulence*, Phys. Fluids **10** (1967), 1417–1423

[5] G. Boffetta and R. E. Ecke, *Two-Dimensional Turbulence*, Annual Review of Fluid Mechanics **44** (2012), 427–451

[6] L. Onsager, *Statistical hydrodynamics*, Il Nuovo Cimento **6** (1949), 279–287

[7] G. L. Eyink and K. R. Sreenivasan, *Onsager and the theory of hydrodynamic turbulence*, Rev. Mod. Phys. **78** (2006), 87–135

[8] G. Joyce and D. Montgomery, *Negative temperature states for the two-dimensional guiding-centre plasma*, Journal of Plasma Physics **10(1)** (1973), 107–121

[9] D. Montgomery and G. Joyce, *Statistical mechanics of 'negative temperature' states*, Phys. Fluids **17** (1974), 1139–1145

[10] C. Bardos, *Existence et unicité de la solution de l'équation d'Euler en dimension deux*, J. Math. Anal. Appl. **40** (1972), 769–790

[11] C. Marchioro and M. Pulvirenti, *Mathematical Theory of Incompressible Nonviscous Fluids*, Springer, New York (1994)

[12] C. Marchioro and M. Pulvirenti, *Vortices and localization in Euler flows*, Comm. Math. Phys. **154** (1993), no. 1, 49–61

[13] R. R. Trieling, O. U. Velasco Fuentes, and G. J. F. van Heijst, *Interaction of two unequal corotating vortices*, Phys. Fluids **17** (2005), 1–17

[14] J. P. Sethna, *Entropy, Order Parameters, and Complexity*, Oxford University Press. (2020)

[15] J. Bedrossian, M. C. Zelati and V. Vicol, *Vortex Axisymmetrization, Inviscid Damping, and Vorticity Depletion in the Linearized 2D Euler Equations*, Ann. PDE **5** (2019)

Appendix A

The Taylor expansions of terms in equation (3.9) (3.10)

Table A.1: Expansion of u^x_{out} and u^y_{out} with coefficient M_x

$-\frac{2(x-i)(y-j)}{((x-i)^2+(y-j)^2)^2}$	$\sum_{\substack{\text{or } \lvert j\rvert>K}} \lvert i\rvert>K$	power
$-\frac{2ij}{(i^2+j^2)^2}$	0	1
$\frac{2j(-3i^2+j^2)}{(i^2+j^2)^3}$	0	x
$\frac{2i(i^2-3j^2)}{(i^2+j^2)^3}$	0	y
$\frac{12ij(-i^2+j^2)}{(i^2+j^2)^4}$	0	x^2
$\frac{6(i^4-6i^2j^2+j^4)}{(i^2+j^2)^4}$	18.90727 $-\sum_{\substack{\lvert i\rvert\leq K\\ \lvert j\rvert\leq K}} \frac{6(i^4-6i^2j^2+j^4)}{(i^2+j^2)^4}$	xy
$\frac{12ij(i^2-j^2)}{(i^2+j^2)^4}$	0	y^2

$-\frac{4j(5i^4-10i^2j^2+j^4)}{(i^2+j^2)^5}$	0	x^3
$\frac{12i(-10i^2j^2+i^4+5j^4)}{(i^2+j^2)^5}$	0	x^2y
$\frac{12j(5i^4-10i^2j^2+j^4)}{(i^2+j^2)^5}$	0	xy^2
$-\frac{4i(i^4-10i^2j^2+5j^4)}{(i^2+j^2)^5}$	0	y^3
...	...	...

$\frac{(x-i)^2-(y-j)^2}{((x-i)^2+(y-j)^2)^2}$	$\sum_{\substack{\text{or } \lvert i\rvert>K \\ \text{or } \lvert j\rvert>K}}$	power
$\frac{i^2-j^2}{(i^2+j^2)^2}$	0	1
$\frac{2i(i^2-3j^2)}{(i^2+j^2)^3}$	0	x
$-\frac{2j(j^2-3i^2)}{(i^2+j^2)^3}$	0	y
$\frac{3(i^4-6i^2j^2+j^4)}{(i^2+j^2)^4}$	9.45364 $-\sum_{\substack{\lvert i\rvert\leq K \\ \lvert j\rvert\leq K}} \frac{3(i^4-6i^2j^2+j^4)}{(i^2+j^2)^4}$	x^2
$\frac{24ij(i^2-j^2)}{(i^2+j^2)^4}$	0	xy
$-\frac{3(i^4-6i^2j^2+j^4)}{(i^2+j^2)^4}$	-9.45364 $+\sum_{\substack{\lvert i\rvert\leq K \\ \lvert j\rvert\leq K}} \frac{3(i^4-6i^2j^2+j^4)}{(i^2+j^2)^4}$	y^2
$\frac{4i(i^4-10i^2j^2+5j^4)}{(i^2+j^2)^5}$	0	x^3
$\frac{12j(5i^4-10i^2j^2+j^4)}{(i^2+j^2)^5}$	0	x^2y
$-\frac{12i(i^4-10j^2i^2+5j^4)}{(i^2+j^2)^5}$	0	xy^2

$-\frac{4j(5i^4-10i^2j^2+j^4)}{(i^2+j^2)^5}$	0	y^3
...	...	...

Table A.2: Expansion of u^x_{out} and u^y_{out} with coefficient M_y

$\frac{(x-i)^2-(y-j)^2}{((x-i)^2+(y-j)^2)^2}$	$\sum_{\substack{\text{or } \lvert i\rvert>K \\ \text{or } \lvert j\rvert>K}}$	power
$\frac{i^2-j^2}{(i^2+j^2)^2}$	0	1
$\frac{2i(i^2-3j^2)}{(i^2+j^2)^3}$	0	x
$-\frac{2j(j^2-3i^2)}{(i^2+j^2)^3}$	0	y
$\frac{3(i^4-6i^2j^2+j^4)}{(i^2+j^2)^4}$	9.45364 $-\sum_{\substack{\lvert i\rvert\le K \\ \lvert j\rvert\le K}} \frac{3(i^4-6i^2j^2+j^4)}{(i^2+j^2)^4}$	x^2
$\frac{24ij(i^2-j^2)}{(i^2+j^2)^4}$	0	xy
$-\frac{3(i^4-6i^2j^2+j^4)}{(i^2+j^2)^4}$	-9.45364 $+\sum_{\substack{\lvert i\rvert\le K \\ \lvert j\rvert\le K}} \frac{3(i^4-6i^2j^2+j^4)}{(i^2+j^2)^4}$	y^2
$\frac{4i(i^4-10i^2j^2+5j^4)}{(i^2+j^2)^5}$	0	x^3
$\frac{12j(5i^4-10i^2j^2+j^4)}{(i^2+j^2)^5}$	0	x^2y
$-\frac{12i(i^4-10j^2i^2+5j^4)}{(i^2+j^2)^5}$	0	xy^2
$-\frac{4j(5i^4-10i^2j^2+j^4)}{(i^2+j^2)^5}$	0	y^3

...	...	...

$\frac{2(x-i)(y-j)}{((x-i)^2+(y-j)^2)^2}$	$\sum_{\substack{\text{or } \lvert i\rvert>K \\ \text{or } \lvert j\rvert>K}}$	power
$\frac{2ij}{(i^2+j^2)^2}$	0	1
$-\frac{2j(-3i^2+j^2)}{(i^2+j^2)^3}$	0	x
$-\frac{2i(i^2-3j^2)}{(i^2+j^2)^3}$	0	y
$-\frac{12ij(-i^2+j^2)}{(i^2+j^2)^4}$	0	x^2
$-\frac{6(i^4-6i^2j^2+j^4)}{(i^2+j^2)^4}$	-18.90727 $+\sum_{\substack{\lvert i\rvert\leq K \\ \lvert j\rvert\leq K}} \frac{6(i^4-6i^2j^2+j^4)}{(i^2+j^2)^4}$	xy
$-\frac{12ij(i^2-j^2)}{(i^2+j^2)^4}$	0	y^2
$\frac{4j(5i^4-10i^2j^2+j^4)}{(i^2+j^2)^5}$	0	x^3
$-\frac{12i(-10i^2j^2+i^4+5j^4)}{(i^2+j^2)^5}$	0	x^2y
$-\frac{12j(5i^4-10i^2j^2+j^4)}{(i^2+j^2)^5}$	0	xy^2
$\frac{4i(i^4-10i^2j^2+5j^4)}{(i^2+j^2)^5}$	0	y^3
...	...	...

Table A.3: Expansion of u^x_{out} and u^y_{out} with coefficient M_{x^2}

$\frac{(y-j)(-3(x-i)^2+(y-j)^2)}{((x-i)^2+(y-j)^2)^3}$	$\sum_{\substack{\text{or } \lvert i\rvert>K \\ \text{or } \lvert j\rvert>K}}$	power
$-\frac{j(j^2-3i^2)}{(i^2+j^2)^3}$	0	1
$-\frac{12ij(j^2-i^2)}{(i^2+j^2)^4}$	0	x
$-\frac{3(i^4-6i^2j^2+j^4)}{(i^2+j^2)^4}$	-9.45364 $+\sum_{\substack{\lvert i\rvert\leq K \\ \lvert j\rvert\leq K}} \frac{3(i^4-6i^2j^2+j^4)}{(i^2+j^2)^4}$	y
$\frac{6j(-10i^2j^2+5i^4+j^4)}{(i^2+j^2)^5}$	0	x^2
$-\frac{12i(-10i^2j^2+i^4+5j^4)}{(i^2+j^2)^5}$	0	xy
$-\frac{6j(-10i^2j^2+5i^4+j^4)}{(i^2+j^2)^5}$	0	y^2
...	...	...

$\frac{(x-i)((x-i)^2-3(y-j)^2)}{((x-i)^2+(y-j)^2)^3}$	$\sum_{\substack{\text{or } \lvert i\rvert>K \\ \text{or } \lvert j\rvert>K}}$	power
$-\frac{i(i^2-3j^2)}{(i^2+j^2)^3}$	0	1
$-\frac{3(i^4-6i^2j^2+j^4)}{(i^2+j^2)^4}$	-9.45364 $+\sum_{\substack{\lvert i\rvert\leq K \\ \lvert j\rvert\leq K}} \frac{3(i^4-6i^2j^2+j^4)}{(i^2+j^2)^4}$	x
$-\frac{12ij(i^2-j^2)}{(i^2+j^2)^4}$	0	y
$-\frac{6i(-10i^2j^2+i^4+5j^4)}{(i^2+j^2)^5}$	0	x^2
$-\frac{12j(-10i^2j^2+5i^4+j^4)}{(i^2+j^2)^5}$	0	xy

$\frac{6i(-10i^2j^2+i^4+5j^4)}{(i^2+j^2)^5}$	0	y^2
...	...	...

Table A.4: Expansion of u^x_{out} and u^y_{out} with coefficient M_{xy}

$\frac{2(x-i)((x-i)^2-3(y-j)^2)}{((x-i)^2+(y-j)^2)^3}$	$\sum_{\substack{\text{or } \lvert i\rvert>K \\ \text{or } \lvert j\rvert>K}}$	power
$-\frac{2i(i^2-3j^2)}{(i^2+j^2)^3}$	0	1
$-\frac{6(i^4-6i^2j^2+j^4)}{(i^2+j^2)^4}$	-18.90727 $+\sum_{\substack{\lvert i\rvert\leq K \\ \lvert j\rvert\leq K}} \frac{6(i^4-6i^2j^2+j^4)}{(i^2+j^2)^4}$	x
$-\frac{24ij(i^2-j^2)}{(i^2+j^2)^4}$	0	y
$-\frac{12i(-10i^2j^2+i^4+5j^4)}{(i^2+j^2)^5}$	0	x^2
$-\frac{24j(-10i^2j^2+5i^4+j^4)}{(i^2+j^2)^5}$	0	xy
$\frac{12i(-10i^2j^2+i^4+5j^4)}{(i^2+j^2)^5}$	0	y^2
...	...	...

$\frac{2(y-j)(3(x-i)^2-(y-j)^2)}{((x-i)^2+(y-j)^2)^3}$	$\sum_{\substack{\text{or } \lvert i\rvert>K \\ \text{or } \lvert j\rvert>K}}$	power
$\frac{2j(j^2-3i^2)}{(i^2+j^2)^3}$	0	1
$\frac{24ij(j^2-i^2)}{(i^2+j^2)^4}$	0	x

$\frac{6(i^4-6i^2j^2+j^4)}{(i^2+j^2)^4}$	18.90727 $-\sum_{\substack{\lvert i\rvert\leq K\\ \lvert j\rvert\leq K}} \frac{6(i^4-6i^2j^2+j^4)}{(i^2+j^2)^4}$	y
$-\frac{12j(-10i^2j^2+5i^4+j^4)}{(i^2+j^2)^5}$	0	x^2
$\frac{24i(-10i^2j^2+i^4+5j^4)}{(i^2+j^2)^5}$	0	xy
$\frac{12j(-10i^2j^2+5i^4+j^4)}{(i^2+j^2)^5}$	0	y^2
...	...	...

Table A.5: Expansion of u^x_{out} and u^y_{out} with coefficient M_{y^2}

$-\frac{(y-j)(-3(x-i)^2+(y-j)^2)}{((x-i)^2+(y-j)^2)^3}$	$\sum_{\substack{\lvert i\rvert>K\\ \text{or } \lvert j\rvert>K}}$	power
$\frac{j(j^2-3i^2)}{(i^2+j^2)^3}$	0	1
$\frac{12ij(j^2-i^2)}{(i^2+j^2)^4}$	0	x
$\frac{3(i^4-6i^2j^2+j^4)}{(i^2+j^2)^4}$	9.45364 $-\sum_{\substack{\lvert i\rvert\leq K\\ \lvert j\rvert\leq K}} \frac{3(i^4-6i^2j^2+j^4)}{(i^2+j^2)^4}$	y
$-\frac{6j(-10i^2j^2+5i^4+j^4)}{(i^2+j^2)^5}$	0	x^2
$\frac{12i(-10i^2j^2+i^4+5j^4)}{(i^2+j^2)^5}$	0	xy
$\frac{6j(-10i^2j^2+5i^4+j^4)}{(i^2+j^2)^5}$	0	y^2
...	...	...

$-\frac{(x-i)((x-i)^2-3(y-j)^2)}{((x-i)^2+(y-j)^2)^3}$	$\sum_{\substack{\text{or } \lvert i\rvert>K \\ \text{or } \lvert j\rvert>K}}$	power
$\frac{i(i^2-3j^2)}{(i^2+j^2)^3}$	0	1
$\frac{3(i^4-6i^2j^2+j^4)}{(i^2+j^2)^4}$	9.45364 $-\sum_{\substack{\lvert i\rvert\leq K \\ \lvert j\rvert\leq K}} \frac{3(i^4-6i^2j^2+j^4)}{(i^2+j^2)^4}$	x
$\frac{12ij(i^2-j^2)}{(i^2+j^2)^4}$	0	y
$\frac{6i(-10i^2j^2+i^4+5j^4)}{(i^2+j^2)^5}$	0	x^2
$\frac{12j(-10i^2j^2+5i^4+j^4)}{(i^2+j^2)^5}$	0	xy
$-\frac{6i(-10i^2j^2+i^4+5j^4)}{(i^2+j^2)^5}$	0	y^2
...	...	...

Table A.6: Expansion of u^x_{out} and u^y_{out} with coefficient M_{x^3}

$-\frac{4(x-i)(y-j)((x-i)^2-(y-j)^2)}{((x-i)^2+(y-j)^2)^4}$	$\sum_{\substack{\text{or } \lvert i\rvert>K \\ \text{or } \lvert j\rvert>K}}$	power
$-\frac{ij(i^2-j^2)}{(i^2+j^2)^4}$	0	1
$-\frac{j(-10i^2j^2+5i^4+j^4)}{(i^2+j^2)^5}$	0	x
$\frac{i(-10i^2j^2+i^4+5j^4)}{(i^2+j^2)^5}$	0	y

...	...	...

$\frac{(x-i)^4-6(x-i)(y-j)^2+(y-j)^2}{((x-i)^2+(y-j)^2)^4}$	$\sum_{\substack{\text{or } \lvert i\rvert>K \\ \text{or } \lvert j\rvert>K}}$	power
$\frac{i^4-6i^2j^2+j^4}{(i^2+j^2)^4}$	$3.15121 - \sum_{\substack{\lvert i\rvert\leq K \\ \lvert j\rvert\leq K}} \frac{(i^4-6i^2j^2+j^4)}{(i^2+j^2)^4}$	1
$\frac{4i(-10i^2j^2+i^4+5j^4)}{(i^2+j^2)^5}$	0	x
$\frac{4j(-10i^2j^2+5i^4+j^4)}{(i^2+j^2)^5}$	0	y
...	...	...

Table A.7: Expansion of u^x_{out} and u^y_{out} with coefficient M_{x^2y}

$\frac{3((x-i)^4-6(x-i)(y-j)^2+(y-j)^2)}{((x-i)^2+(y-j)^2)^4}$	$\sum_{\substack{\text{or } \lvert i\rvert>K \\ \text{or } \lvert j\rvert>K}}$	power
$\frac{3(i^4-6i^2j^2+j^4)}{(i^2+j^2)^4}$	$9.45364 - \sum_{\substack{\lvert i\rvert\leq K \\ \lvert j\rvert\leq K}} \frac{3(i^4-6i^2j^2+j^4)}{(i^2+j^2)^4}$	1
$\frac{12i(-10i^2j^2+i^4+5j^4)}{(i^2+j^2)^5}$	0	x
$\frac{12j(-10i^2j^2+5i^4+j^4)}{(i^2+j^2)^5}$	0	y
...	...	...

$\frac{12(x-i)(y-j)((x-i)^2-(y-j)^2)}{((x-i)^2+(y-j)^2)^4}$	$\sum_{\substack{\text{or } \lvert i\rvert>K \\ \text{or } \lvert j\rvert>K}}$	power

$\frac{3ij(i^2-j^2)}{(i^2+j^2)^4}$	0	1
$\frac{3j(-10i^2j^2+5i^4+j^4)}{(i^2+j^2)^5}$	0	x
$-\frac{3i(-10i^2j^2+i^4+5j^4)}{(i^2+j^2)^5}$	0	y
...	...	...

Table A.8: Expansion of u^x_{out} and u^y_{out} with coefficient M_{xy^2}

$\frac{12(x-i)(y-j)((x-i)^2-(y-j)^2)}{((x-i)^2+(y-j)^2)^4}$	$\sum_{\substack{\text{or } \lvert i\rvert>K \\ \text{or } \lvert j\rvert>K}}$	power
$\frac{3ij(i^2-j^2)}{(i^2+j^2)^4}$	0	1
$\frac{3j(-10i^2j^2+5i^4+j^4)}{(i^2+j^2)^5}$	0	x
$-\frac{3i(-10i^2j^2+i^4+5j^4)}{(i^2+j^2)^5}$	0	y
...	...	...
$-\frac{3((x-i)^4-6(x-i)(y-j)^2+(y-j)^2)}{((x-i)^2+(y-j)^2)^4}$	$\sum_{\substack{\text{or } \lvert i\rvert>K \\ \text{or } \lvert j\rvert>K}}$	power
$-\frac{3(i^4-6i^2j^2+j^4)}{(i^2+j^2)^4}$	-9.45364 $+\sum_{\substack{\lvert i\rvert\leq K \\ \lvert j\rvert\leq K}} \frac{3(i^4-6i^2j^2+j^4)}{(i^2+j^2)^4}$	1
$-\frac{12i(-10i^2j^2+i^4+5j^4)}{(i^2+j^2)^5}$	0	x

$-\frac{12j(-10i^2j^2+5i^4+j^4)}{(i^2+j^2)^5}$	0	y
...	...	...

Table A.9: Expansion of u^x_{out} and u^y_{out} with coefficient M_{y^3}

$-\frac{(x-i)^4-6(x-i)(y-j)^2+(y-j)^2}{((x-i)^2+(y-j)^2)^4}$	$\sum_{\text{or } \lvert j\rvert>K}^{\lvert i\rvert>K}$	power
$-\frac{i^4-6i^2j^2+j^4}{(i^2+j^2)^4}$	-3.15121 $+\sum_{\substack{\lvert i\rvert\le K\\ \lvert j\rvert\le K}} \frac{(i^4-6i^2j^2+j^4)}{(i^2+j^2)^4}$	1
$-\frac{4i(-10i^2j^2+i^4+5j^4)}{(i^2+j^2)^5}$	0	x
$-\frac{4j(-10i^2j^2+5i^4+j^4)}{(i^2+j^2)^5}$	0	y
...	...	...

$-\frac{4(x-i)(y-j)((x-i)^2-(y-j)^2)}{((x-i)^2+(y-j)^2)^4}$	$\sum_{\text{or } \lvert j\rvert>K}^{\lvert i\rvert>K}$	power
$-\frac{ij(i^2-j^2)}{(i^2+j^2)^4}$	0	1
$-\frac{j(-10i^2j^2+5i^4+j^4)}{(i^2+j^2)^5}$	0	x
$\frac{i(-10i^2j^2+i^4+5j^4)}{(i^2+j^2)^5}$	0	y
...	...	...

Table A.10: Expansion of u^x_{out} and u^y_{out} with coefficient M_{x^4}

$-\frac{(y-j)(-10(x-i)^2(y-j)^2+5(x-i)^4+(y-j)^4)}{((x-i)^2+(y-j)^2)^5}$	$\sum_{\substack{\text{or } \lvert i\rvert>K \\ \text{or } \lvert j\rvert>K}}$	power
$\frac{j(-10i^2j^2+5i^4+j^4)}{(i^2+j^2)^5}$	0	1
...	...	...
$\frac{(x-i)(-10(x-i)^2(y-j)^2+(x-i)^4+5(y-j)^4)}{((x-i)^2+(y-j)^2)^5}$	$\sum_{\substack{\text{or } \lvert i\rvert>K \\ \text{or } \lvert j\rvert>K}}$	power
$-\frac{i(-10i^2j^2+i^4+5j^4)}{(i^2+j^2)^5}$	0	1
...	...	...

Table A.11: Expansion of u^x_{out} and u^y_{out} with coefficient M_{x^3y}

$\frac{4(x-i)(-10(x-i)^2(y-j)^2+(x-i)^4+5(y-j)^4)}{((x-i)^2+(y-j)^2)^5}$	$\sum_{\substack{\text{or } \lvert i\rvert>K \\ \text{or } \lvert j\rvert>K}}$	power
$-\frac{4i(-10i^2j^2+i^4+5j^4)}{(i^2+j^2)^5}$	0	1
...	...	...
$\frac{4(y-j)(-10(x-i)^2(y-j)^2+5(x-i)^4+(y-j)^4)}{((x-i)^2+(y-j)^2)^5}$	$\sum_{\substack{\text{or } \lvert i\rvert>K \\ \text{or } \lvert j\rvert>K}}$	power

$-\frac{4j(-10i^2j^2+5i^4+j^4)}{(i^2+j^2)^5}$	0	1
...	...	...

Table A.12: Expansion of u^x_{out} and u^y_{out} with coefficient $M_{x^2y^2}$

$\frac{6(y-j)(-10(x-i)^2(y-j)^2+5(x-i)^4+(y-j)^4)}{((x-i)^2+(y-j)^2)^5}$	$\sum_{\substack{\text{or } \lvert j\rvert>K}} \lvert i\rvert>K$	power
$-\frac{6j(-10i^2j^2+5i^4+j^4)}{(i^2+j^2)^5}$	0	1
...	...	...
$-\frac{6(x-i)(-10(x-i)^2(y-j)^2+(x-i)^4+5(y-j)^4)}{((x-i)^2+(y-j)^2)^5}$	$\sum_{\substack{\text{or } \lvert j\rvert>K}} \lvert i\rvert>K$	power
$\frac{6i(-10i^2j^2+i^4+5j^4)}{(i^2+j^2)^5}$	0	1
...	...	...

Table A.13: Expansion of u^x_{out} and u^y_{out} with coefficient M_{xy^3}

$-\frac{4(x-i)(-10(x-i)^2(y-j)^2+(x-i)^4+5(y-j)^4)}{((x-i)^2+(y-j)^2)^5}$	$\sum_{\substack{\text{or } \lvert j\rvert>K}} \lvert i\rvert>K$	power

$\frac{4i(-10i^2j^2+i^4+5j^4)}{(i^2+j^2)^5}$	0	1
...	...	...
$-\frac{4(y-j)(-10(x-i)^2(y-j)^2+5(x-i)^4+(y-j)^4)}{((x-i)^2+(y-j)^2)^5}$	$\sum_{\substack{\text{or } \lvert j\rvert>K}}^{\lvert i\rvert>K}$	power
$\frac{4j(-10i^2j^2+5i^4+j^4)}{(i^2+j^2)^5}$	0	1
...	...	...

Table A.14: Expansion of u^x_{out} and u^y_{out} with coefficient M_{y^4}

$-\frac{(y-j)(-10(x-i)^2(y-j)^2+5(x-i)^4+(y-j)^4)}{((x-i)^2+(y-j)^2)^5}$	$\sum_{\substack{\text{or } \lvert j\rvert>K}}^{\lvert i\rvert>K}$	power
$\frac{j(-10i^2j^2+5i^4+j^4)}{(i^2+j^2)^5}$	0	1
...	...	...
$\frac{(x-i)(-10(x-i)^2(y-j)^2+(x-i)^4+5(y-j)^4)}{((x-i)^2+(y-j)^2)^5}$	$\sum_{\substack{\text{or } \lvert j\rvert>K}}^{\lvert i\rvert>K}$	power
$-\frac{i(-10i^2j^2+i^4+5j^4)}{(i(x-i)^2+i)^2)^5}$	0	1
...	...	...

Appendix B

Figures of evolution of 2D turbulence

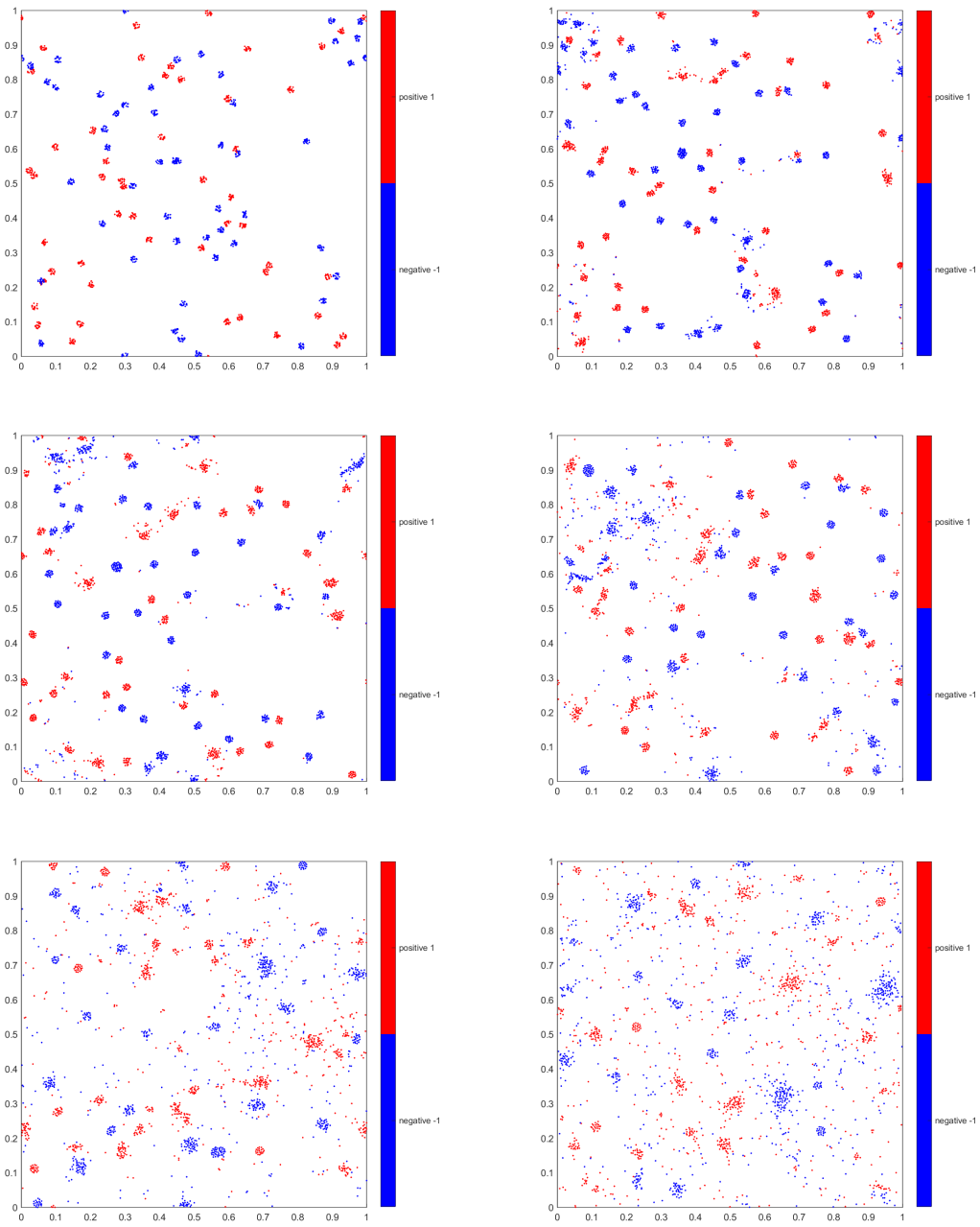

Figure B.1: 2D turbulence on torus, at time 0, 1, 2, 5, 10, 20

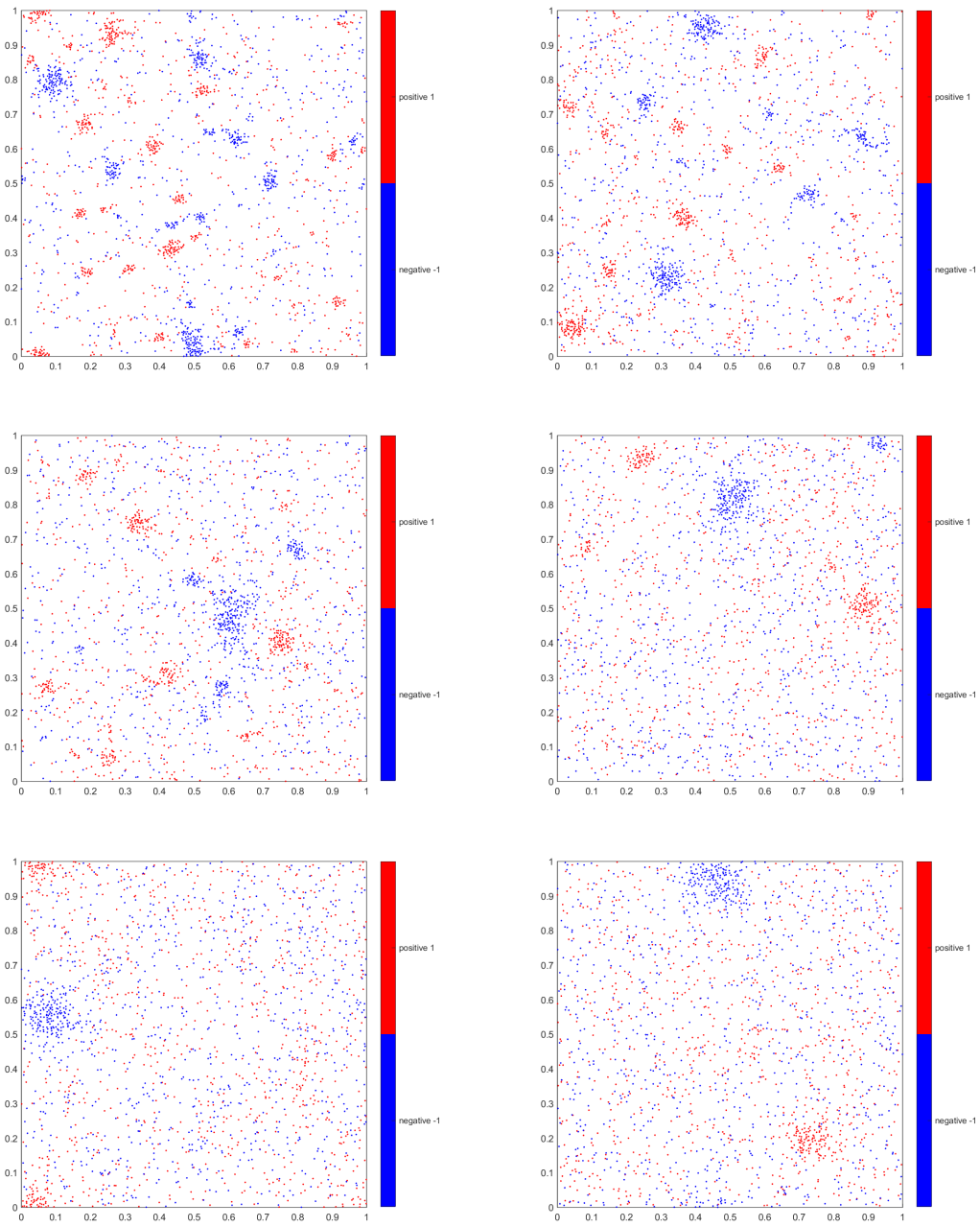

Figure B.2: 2D turbulence on torus, at time 30, 40, 50, 100, 150, 200